Hydrol. Earth Syst. Sci. Discuss., https://doi.org/10.5194/hess-2019-116
Manuscript under review for journal Hydrol. Earth Syst. Sci.
Discussion started: 2 May 2019

Hydrology and Earth System Sciences
Discussions

A non-stationary model for reconstruction of historical annual runoff on tropical catchments under increasing urbanization (Yaoundé, Cameroon)

Camille Jourdan[1,2], Valérie Borrell-Estupina[3], David Sebag[4], Jean-Jacques Braun[5,6], Jean-Pierre Bedimo Bedimo[6,†], François Colin[2], Armand Crabit[2], Alain Fezeu[7], Cécile Llovel[8], Jules Rémy Ndam Ngoupayou[9], Benjamin Ngounou Ngatcha[10], Sandra Van-Exter[11], Eric Servat[1], Roger Moussa[2]

[1] OSU OREME, Univ Montpellier, Montpellier, France

[2] LISAH, Univ Montpellier, INRA, IRD, SupAgro, Montpellier, France

[3] HSM, Univ Montpellier, CNRS, IRD, Montpellier, France

[4] Normandie Univ, UNIROUEN, UNICAEN, CNRS, M2C, Rouen, France

[5] GET, CNRS, IRD, University of Toulouse, Toulouse, France

[6] Institut de Recherches Géologiques et Minières, Centre de Recherches Hydrologiques, Yaoundé, Cameroon

[7] French National Research Institute for Development (IRD), Yaoundé, Cameroon

[8] WSP France, Toulouse, France

[9] Laboratoire de Géologie de l'ingénieur et d'Altérologie, Département des Sciences de la Terre et de l'Univers, Faculté des Sciences, Université de Yaoundé I, BP 812, Yaoundé, Cameroun

[10] Department of Earth Sciences, Faculty of Sciences, University of Ngaoundéré, Ngaoundere, Cameroon

[11] GM, Univ Montpellier, CNRS, Université des Antilles, Montpellier, France

[†] deacesed

Correspondence: Camille Jourdan (camille.jourdan@umontpellier.fr)

Hydrol. Earth Syst. Sci. Discuss., https://doi.org/10.5194/hess-2019-116
Manuscript under review for journal Hydrol. Earth Syst. Sci.
Discussion started: 2 May 2019

Hydrology and Earth System Sciences
Discussions

Abstract. Inter-tropical regions are nowadays faced to major land-use changes in data-sparse context leading to difficulties to assess hydrological signatures and their evolution. This work is part of the theme *Panta Rhei* of the IAHS, and aims to develop a combined approach of data acquisition and a new semi-distributed model taking into account land-use changes to reconstruct and predict annual runoff on an urban catchment. Applications were conducted on the Mefou catchment at Nsimalen (421 km²; Yaoundé, Cameroon) under rapid increase in urbanization since 1960. The data acquisition step combines an historical data processing and a short-term spatially-dense dedicated instrumentation (2017-2018), leading to 12 donor catchments, 6 from historical studies and 6 from the instrumentation presenting various topographic, soil and land-use characteristics. We developed an annual rainfall-runoff model based on mathematical relationships similar to the SCS model. The model needs the definition of a hydrological index I which is time variable and enables to take into account land-use changes and non-stationary relationships between rainfall and runoff. The index I is an empirical indicator defined as a combination of several components such as topography, soil, and land-use. The rules for the construction of I are obtained from data analysis on donor catchments. Then, the model was calibrated on donor catchments. Finally, two applications were conducted on eight target catchments composing the Mefou in order: i) to study the spatial hydrological functioning and calculate the water balance during the short instrumentation period; ii) to reconstruct the hydrograph at the Mefou and to simulate the impact of future scenarios of land-use and urbanization. Results show that that the Mfoundi catchment, integrating the three more urbanized sub-catchments, contributes near to 40 % of the Mefou despite covering only 23 % of the basin. The most urbanized sub-catchments present annual runoff coefficient about 0.86 against 0.24 for the most natural sub-catchments. The second result is the reconstruction of historical annual runoff from 1930-2017 with r^2 = 0.68, $RMSE$ = 99 mm and a mean absolute normalized error $\bar{E}$ = 14.5 % over the 29 observed years. The reconstruction of the annual runoff at Nsimalen confirms the moderate impact of urbanization on annual runoff before 1980. However, a decrease of about 50 % of the forest cover and an increase from 10 % to 35 % of the urban area between 1980 and 2017 are associated with an increase of 53 % of annual runoff coefficient for the Mefou at Nsimalen (0.44 against 0.29). Application for a fictive plausible scenario of urbanization in 2030 leads to an increase of more than 85 % of the annual runoff in comparison of the values observed in 1980. The coupled experimental-modelling approach proposed herein opens promising perspectives regarding the evaluation of the annual runoff in catchments under changes.

Hydrol. Earth Syst. Sci. Discuss., https://doi.org/10.5194/hess-2019-116
Manuscript under review for journal Hydrol. Earth Syst. Sci.
Discussion started: 2 May 2019

1 Introduction

The link between the hydrological cycle and human societies has been strong with changes and intensification of these interactions over time (Koutsoyiannis, 2013; McMillan et al., 2016). In response to the imperative to include human increasing impacts as integral to hydrological research, the International Association of Hydrological Sciences (*IAHS*) launched the hydrological decade (2013-2022) with theme "*Panta Rhei: Change in Hydrology and Society*". Due to rapid and complex anthropic changes, the *IAHS* emphasize the necessity to improve the capability of decision maker and water resources stakeholders to make predictions of hydrological dynamics and support sustainable societal development in a changing environment (Montanari et al., 2013). Quantifying and understanding past changes in hydrological processes are necessary to suggest reliable future predictions of hydrological signatures. Reconstructing past data and predicting annual, monthly and daily hydrographs in a changing environment, and especially on poorly gauged catchments with sparse data, remains a challenge for hydrological science.

Long-term hydrological modelling requires integrating the impact of global changes in terms of climate, land-use and infrastructures. Nowadays, urban areas represent only 2 % of the total surface of the Earth but concentrate more than 50 % of world population, cities count close to four billions people, this figure was multiplied by five since 1950 (Janicot et al., 2015). This huge urbanization rate combined with a demographic explosion is especially significant in the inter-tropical regions where most of developing countries and numerous in development megalopolis are located (UNDESA, 2017). For example, population in Africa is projected to reach 2.5 billion people by 2050 with about 55 % living in urban areas (Güneralp et al., 2017). Hence in this context, the impact of land-use changes on runoff, especially in urban and peri-urban zones, seems to override rainfall changes impacts.

Empirical, conceptual, probabilistic and physically-based models can be used to simulate the impact on runoff of global changes. Conceptual models such as *HBV* (Bergström and Singh, 1995), *GR1A*, *GR2M* or *GR5J* (Mouelhi, 2003; Mouelhi et al., 2006; Le Moine, 2008) or physically-based models as *MIKE-SHE* (Abbott et al., 1986) were applied to assess global changes impacts on hydrology. On tropical climate, such models were applied at the local scale (Giertz et al., 2006), the mesoscale (Beck et al., 2013; Wagner et al., 2013; Yira et al., 2016) or large scale catchments (Genwei, 1999; Zhou et al., 2010) at daily, monthly or annual time steps. All these models require accurate information about the basin physiographic characteristics, long series of rainfall-runoff data, climate and land-use changes data; moreover an adequate calibration/validation strategy must be undertaken in order to take into account the spatio-temporal evolution of some parameters. However, on basins with sparse data at various time steps (e.g. only monthly rainfall available on a given period), and in the absence of continuous long series rainfall-runoff data, simple modelling approaches must be adapted for reconstructing annual runoff taking into account available sparse historical data and information on climate and land-use changes. For that, empirical approaches in non-dimensional spaces were largely used since Turc (1954) and Budyko (1974) which were largely applied, analysed and extended the last decade (Zhou et al., 2015; see a synthesis in Moussa and Lhomme, 2016). Ponce and Shetty (1995) developed an original annual rainfall-runoff model based on a formulation similar to the one developed in the Soil Conservation Service method (SCS, 1956; Mishra and Singh, 2013), and Sivapalan et al. (2011) extended this approach to model different components of the water cycle at the annual scale. However, all these models generally don't take into account changes in climate

and land-use. Hence, there is a need to develop simple parsimonious approaches modelling for annual runoff taking into account non-stationarity due to land-use long term evolution, and adapted to basins with sparse data.

In most of developing countries, environmental monitoring as precipitation and streamflow are often limited. This data-sparse condition results of a poor knowledge of basin climatology and hydrological signatures, such as annual runoff. Even for areas faced with recurring high water management issues, most of national organizations do not have resources to purchase and maintain the necessary instrumentation for field monitoring (Hughes et al., 2015). The availability of continuous and long term data sets of runoff varies dramatically throughout the world (Kundzewicz et al., 2007). Prediction in ungauged basins (*PUB*) approaches are tools to cope with this data-sparse context (Blöschl, 2013) and are based on regionalization of hydrological characteristics by spatial proximity or geomorphological similarities from donor to target catchments (Parajka et al., 2013; Salinas et al., 2013). However, recently development of soft monitoring (Crabit et al., 2011) and crowdsourced hydrology (Lowry and Fienen, 2013; Le Coz et al., 2016; Mazzoleni et al., 2017) gave encouraging results. To cope with the lack of long-term observation (rainfall-runoff) on catchment faced to land-use changes a solution is to set up a dedicated short-term instrumentation on catchment faced to various land-use states associated with a best valorisation of historical database. This methodology lets to observe hydrological processes of catchments characterized by various states of land-use and under various climatic contexts.

The scope of this paper is to develop a combined approach of data acquisition and the development of a new semi-distributed model taking into account land-use changes to reconstruct and predict annual runoff on a catchment exposed to high urban increase. The data acquisition step implies (1) to deploy a complementary and dedicated short-term and multi-scale space hydro-meteorological network, (2) to analyse the most recent global land-use products with adapted time and space resolution and (3) to maximize the valorisation of historical studies for the evaluation of catchment characteristics (land-use, topography, soils map) and some environment variables (evaporation, precipitation, runoff). The model developed from the data acquisition is mainly based on land-use changes impacts on annual runoff.

The Mefou catchment (421 km²) including the city of Yaoundé capital of Cameroon was used for applications to reconstruct the annual runoff at the outlet for the period 1930-2017. A dedicated hydrological instrumentation during the hydrological year 2017-2018 was conducted, and completes the review of historical studies over the period 1960-2016.

First, we introduce the annual non-stationary rainfall-runoff model structure, hypotheses and general calibration-validation procedure. The inputs of the model are the annual precipitation and an hydrologic index taking into account topography, soil and land-use temporal evolution. Second, we describe the study area including the review of historical hydro-meteorological data and a description of the dedicated short-terms instrumentation. Third, we present a spatio-temporal analysis of precipitation. Fourth, we present the methodology to construct the hydrological index from the analysis of hydrologic and physiographic data. Then, we present the model parametrization, calibration and validation, and finally we show and discuss the application results of reconstruction and prediction of historical annual runoff. The Appendix A gives the list of notations and abbreviations. The Su**p**plementary Material gives additional information on data sets.

Hydrol. Earth Syst. Sci. Discuss., https://doi.org/10.5194/hess-2019-116
Manuscript under review for journal Hydrol. Earth Syst. Sci.
Discussion started: 2 May 2019

Hydrology and Earth System Sciences
Discussions

2 The annual rainfall-runoff model

2.1 Model structure

The model is based on mathematical relationship between precipitation P and runoff R similar that proposed by Ponce and Shetty (1995) and Sivapalan et al. (2011) for applications at the annual scale on the basis of the *SCS* equations (Mishra and Singh, 2003). P ranges between P_n and P_x which respectively correspond to the minimal and the maximal precipitation values over a large historical period of the main study catchment. Applications were conducted in tropical basins where R is not nil. Therefore, in order to simplify, we use a simple second order polynomial relationship between R and P such as (Fig.1):

$$R = AP^2 + BP, \quad (1)$$

and the annual runoff coefficient:

$$\rho = R/P = AP + B, \quad (2)$$

where A and B are empirical parameters which can be linked to catchment properties (e.g. topography, soil, land-use).

The first hypothesis is that the annual volume V_O at the outlet of the main catchment is the sum of the annual volumes V_i on each sub-catchment T_i (Fig. 2b):

$$V_O = \sum_{i=1}^{n} V_i , \quad (3)$$

where n is the number of sub-catchments and i is the index representing a sub-catchment noted T_i. We define the annual runoff R_i on each sub-catchment T_i as:

$$R_i = {}^{V_i}/_{A_i} , \quad (4)$$

where A_i is the area of T_i and A_O is the area of the whole catchment with:

$$A_O = \sum_{i=1}^{n} A_i , \quad (5)$$

Consequently the annual runoff R_O of the whole catchment is defined as:

$$R_O = {}^{V_o}/_{A_0} . \quad (6)$$

The second hypothesis presumes that the runoff coefficient $\rho = R / P$ and the annual runoff R are only functions of P and an "hydrological index" noted I with $\rho = f(P, I)$ and $R = g(P, I)$ similar to the SCS approach used in Ponce and Shetty (1995) and Sivapalan et al. (2011). As for the curve numbers *CN* in the Soil Conservation Service method (Mishra and Singh, 2003), the index I characterizes topography, soil and land-use of the basin, and enables to take into account land-use evolution through time: I is considered low for permeable soils and/or low urbanization areas producing low runoff, and I is considered high for impermeable soils and/or high urbanization areas producing high runoff. The index I is an empirical indicator and can be defined as a linear combination of several components C_i. As for the *CN* method, in this study we choose the following three components: topographic component (C_T) such as slope classes impacting runoff, and soil component (C_S) such as permeability classes and land-use component (C_{LC}) such as urbanization classes.

$$I = \sum_{i=1}^{m} \omega_i C_i \,, \quad (7)$$

where ω_i is the weight attributed to component i and m the number of components including in the hydrological index. If m is equal to 1, the hydrological index I is based on only one component, for example the land-use characteristics (C_{LC}) if this descriptor is considered as the main factor changing in time.

We note I_n and I_x respectively the lowest and the highest values of I over the catchment dataset used to construct the model. Therefore, for a given rainfall P, R increases when I increases; for a given index I, R increases when P increases.

For a given value of I the runoff coefficient ρ increases when the rainfall increases from P_n to P_x. Let $\rho_{n,I}$ and $\rho_{x,I}$ be the corresponding values of ρ for P_n and P_x respectively. Let $\beta_1 = \rho_{x,I} - \rho_{n,I}$ as shown in Fig. 1a. For a given value of P, the runoff coefficient ρ increases when I increases from I_n to I_x. Let $\rho_{n,P}$ and $\rho_{x,P}$ be the corresponding values of ρ for I_n and I_x respectively. Let $\beta_2 = \rho_{x,P} - \rho_{n,P}$ as shown in Fig. 1a. As we have a linear relationship between P and ρ (Fig. 1a), the value of β_2 is constant and similar for all values of P. In order to calculate β_2, we need data on different catchments and periods with the same value of P but with different values of I ranging between I_n and I_x.

The annual runoff model proposed herein uses a simple relationship $R = f(P, I)$ as shown in Fig. 1b. The domain of application of the model is for the precipitation $P \in [P_n, P_x]$ and the hydrological index $I \in [I_n, I_x]$. The model needs as input the precipitation P which has to be calculated on each sub-catchment T_i (see an application in Sect. 4). The model needs also the definition of the hydrological index I which is time variable and enables to take into account land-use changes and non-stationary relationships between R and P. The definition of the rules to construct the components C_i and the weights ω_i of I (Eq. 7) are obtained from data analysis on the study site as shown later in Sect. 5.

2.2 Calibration, validation, reconstruction procedure

The annual rainfall-runoff model developed herein is calibrated using data from donor catchments (noted D) historical information, and from the dedicated short-term instrumentation. Donors could be catchments or sub-catchments inside or near to the main study catchment (Fig. 2a). Sets of annual precipitation P and annual runoff R data are available for donors characterized by different geomorphologic and land-use states (e.g. topography, soil, urbanization). Selecting distant past, recent past and present in P and R values from donors enable to cover a large range of climate, land-use and geomorphological conditions in order to elaborate a reliable and robust model. Donors are used to calibrate the model parameters then the calibrated model is applied on target catchments (noted T, Fig. 2b) and let to evaluate runoff for the main catchment (Eq. 3 to 6). The model can be applied for several periods (past, present and future) for different climate and land-use scenarios.

We consider the set of sparse annual rainfall-runoff data. The set is split into two datasets, the first one is used for the calibration of the model parameters and the second one for the validation. The dataset used for the calibration must include data from different ranges of precipitation $P_n < P < P_x$ and land-use characterized by the

hydrological index $I_n < I < I_x$. The *RMSE*, the r^2, the normalised error (E) and the mean normalised absolute error ($\bar{E}$) criteria functions are used to assess and compare simulation performance:

$$RMSE = \sqrt{\frac{1}{n}\sum\left(\widehat{R_{O_j}} - R_{O_j}\right)^2}, \quad (8)$$

$$r^2 = \frac{\left[\sum\left(\widehat{R_{O_j}} - \overline{\widehat{R_O}}\right)\left(R_{O_j} - \overline{R_O}\right)\right]^2}{\sum\left(R_{O_j} - \overline{R_O}\right)^2}, \quad (9)$$

$$E_j = \frac{\widehat{R_{O_j}} - R_{O_j}}{R_{O_j}}, \text{ and } E_{i,j} = \frac{\hat{R}_{i,j} - R_{i,j}}{R_{i,j}}, \quad (10)$$

$$\bar{E} = \frac{1}{n}\sum(|E_j|), \quad (11)$$

where $\widehat{R_{O_j}}$ is the simulated annual runoff and $R_{O\,j}$ the observed annual runoff for the main study catchment; n the number of the evaluated year and j the index corresponding to a given year. $\hat{R}_{i,j}$ is the simulated annual runoff for target i for the evaluated year j and $R_{i,j}$ the observed annual for target i for the evaluated year j. In order to evaluate the robustness of the model, a sensitivity analysis is conducted on the impact of the number of donor catchments used establishing the rules of the hydrologic index I. Finally, the performance of the developed model is compared to a classical annual runoff model generally applied under stationary conditions (i.e. the *GR1A* model based on the Turc (1954) equation; Mouelhi, 2003).

3 Study site

3.1 Oro-hydrography and climate

The Mefou River is a tributary of the Nyong. The Mefou catchment at Nsimalen (421 km²) includes the capital city of Cameroon, Yaoundé (Fig. 3a).The upstream part of the basin (70 km²) is controlled by the Mopfou dam built in 1969 planned to provide about one third of the drinking water to the Yaoundé urban area (100,000 $m^3.day^{-1}$).

The catchment is hilly (peaks at 1000 m a.s.l) with important wetland areas (around 700 m a.s.l) at the downstream parts (Fig. 3a). The Mefou River is 35 km length from the Mopfou dam to Nsimalen. The main tributaries of the Mefou is the Mfoundi which drains the most urbanized parts of the whole catchment (Fig. 3a). The river channel slope ranges between 1 ‰ and 5 ‰ causing frequent floods in the lowlands. Canalization of the upstream Mfoundi and its tributaries were undertaken since 2002 in order to reduce floods in the urbanized zone. The landform of the South Cameroon Plateau corresponds to the dismantling of an old iron crust undergoing more humid climatic conditions (Bilong et al., 1992; Beauvais, 1999; Bitom et al., 2004). This multi-convex landform is composed of rather closely spaced hilly compartments, typically of few hundred metres in diameter, separated by flat swampy valleys of variable stretch from 50 to 500 m width (Bitom et al., 2004). We used the slope index S_I of Roche (Roche, 1963) to characterize the topography component of the hydrological index I for donor and target catchments.

The climate is humid tropical with two dry and wet seasons (wet-and-dry equatorial savannah with dry winter according to the Köppen-Geiger classification, Kottek et al., 2006). The mean annual precipitation P_m from Mvan

station (P_1) in Yaoundé on the period 1930-2015 is 1580 mm. We distinguish four seasons: long rainy season from March to June, short dry season from July to August, short rainy season from September to November, and long dry season from December to February. The hydrological year is defined from March to February. Ikounga (1978) has estimated the potential evapotranspiration *PET* between 900 mm (Sunken Colorado pan) to 1200 mm (Thornthwaite method). Supplementary Material (Sect. 2, Fig. S1) shows the mean monthly precipitation, temperature and *PET*.

3.2 Soil and land-use

The regolith is developed on a granito-gneissic basement. Ferralsol (laterite) regolith is developed on the hillslopes while in the swampy valleys, it is topped with bleached hydromorphic soils developed on colluvium and river alluvium (Bachelier, 1959; Braun et al., 2005; Braun et al., 2012). In the region of Yaoundé, Humbel and Pellier (1969) calculated a soil surface permeability between 20 and 70 $cm.h^{-1}$ up the hill, and 200 $cm.h^{-1}$ near the swampy valleys. These values of permeability are very high and limit the surface runoff, especially in swampy valleys. The clay amount is generally higher at the top of the hills than at the bottom. In the field experiment we conducted in 2017, we measured in the region of Yaoundé the soil surface permeability by a simplified Beerkan method (Bagarello et al., 2014) and obtained values ranging between 2 and 125 $cm.h^{-1}$ which are comparable to the values given by Humbel and Pellier (1969). Humbel and Pellier (1969) also showed that for both types of soil, the surface permeability decreases quickly with the depth until an impermeable layer facilitating lateral flow. In this study we use the proportion of hydromorphic soil (*HS*) to characterize the soil component of the hydrological index *I* for donor and target catchments (see Sect. 5.1).

The administrative urban area of Urban Community of Yaoundé (*CUY*) covers nowadays about 297 km². As most part of the Nyong basin (Olivry, 1979), the Mefou catchment was originally mainly covered by humid tropical forest. The study area is faced to major land-use changes due to human activities mainly urbanization and agriculture (see more details in Supplementary Material, Sect. 3). Population in Yaoundé has increased from 90,000 in 1960 (Franqueville, 1968) to 3.65 million in 2017 (UNDESA, 2017) with an annual growth rate of 5.7 % per year between 1987 and 2005 according to the Central Office of Cameroonian Population Study and Census. This huge demographic change is characterized by an important expansion of the urban area Fig. 3b and the increase of population density (Bopda, 2003). In the opposite, forest and wetlands areas decreased, and were generally replaced by agricultural and urban areas as shown in Fig. 3c with the land-use classification over the Mefou catchment from the land cover product of the European Space Agency available for Africa (*ESA-CCI LC)* for the year 2016. Moffo (2017) analysed a set of aerial photography in 1956 and estimated that the impervious areas covered 3.5 km², less than 1 % of the Mefou catchment area. We used *ESA-CCI LC* and OpenStreetMap® 2015 layers to calculate impervious areas of around 64 km² (15 %) in 2016. Ebodé (2017) used Landsat images to study the evolution of land-use from 1978 to 2015. He noticed at the Mefou catchment until the Nyong confluence (basin area of 802 km², approximately two times the Mefou basin area at Nsimalen) a decrease of 160 km² of the total forest cover, with specifically a decrease of 60 % of the primary forest area from 235 km² in 1978 to 94 km² in 2015, a decrease of 73 % for swampy forest from 206 km² to 57 km², and an increase of 60 % in degraded and secondary forest from 223 km² to 353 km². For the Mefou at Nsimalen, Ebodé (2017) estimated that the agricultural

area increased from 10 km² (3.5 % of the catchment area) in 1978 to 28 km² (10 %) in 2015, and that the urban area (integrating impervious surfaces) increased from 45 km² (11 %) in 1978 to 151 km² (36 %) in 2015. We used the proportion of urban area U over donor and target catchments to characterize the land-use component of the hydrological index.

The impact of these land-use changes on hydrological processes is not yet quantified on the Mefou catchment. The urbanization of the Mefou catchment also impacts both groundwater and river water quality due to domestic and industrial untreated wastewater from urban areas but also contamination by peri-urban agriculture. For example, Branchet et al. (2018) recently shows high Diuron® concentration on surface water that frequently exceeded the European water quality guideline. These growing issues of water management drive the removal of wetlands in lowlands impacting their ecosystem services as the natural purification of water (Daily, 1997; Russo, 2013).

3.3 Historical sparse data

Precipitation measurements are available at a monthly time step at two historical raingauges (Fig. 3a): P_1 from 1930 to 2017, and P_2 from 1955 to 1978. The correlation coefficient for the common period between both stations at the annual time step is 0.74. A long-term reference precipitation dataset was calculated using the mean of P_1 and P_2 when data from both stations are available, and from P_1 for the remaining periods.

Daily runoff measurements at the Mefou catchment outlet at Nsimalen started in 1963 but with long periods of gaps. Annual runoff is available for only 29 years (1964-1977, 1979, 1982-1986, 2005-2011 and 2017), and ranges between 250 mm and 850 mm. Annual runoff coefficient ranges between 0.21 and 0.48.

Few studies are available on the hydrology of Yaoundé, and most of them date before the 80th. They particularly focused on water balance at monthly and annual scales: on the Mefou river (Lefèvre, 1966; SNEC, 1969; Olivry, 1979), on the Mfoundi (Srang, 1972; Nguemou, 2008), and on sites downstream Nsimalen (Ikounga, 1978). From these studies, we retain six historical donors (noted D_H; Fig. 4a), and Table 1 presents their characteristics: area between 24 and 235 km², period of observation, annual precipitation P between 1640 and 1930 mm, annual runoff R between 392 and 1340 mm, and annual runoff coefficient ρ between 0.22 and 0.77. Under the hypothesis that the storage annual variation is nil, we estimate an annual evapotranspiration $AET = P - R$ which ranges between 400 and 1400 mm. Information relative to precipitation measurements are well documented in the historical studies previously cited. Note that the donor D_{H6} is located out of the Mefou catchment but quite close from Yaoundé area (40 km) and presents a similar topography, soil and land-use conditions of the Mefou catchment (Ikounga, 1978). These donors cover different land-use states: e.g. forestry natural cover for D_{H4} and D_{H6} (U < 1%) and highly urbanized cover for D_{H3} (U > 75%).

Other historical studies of smaller (< 10km²) and larger (> 5000 km²) catchments in Nyong basins in natural land-use context give P between 1420 and 1730 mm, R between 392 and 530 mm, ρ between 0.18 and 0.30 and AET between 1070 and 1470 mm. The urbanized catchment Odza (6 km²), located in Yaoundé (Mfoundi

306 catchment), was monitored in 2011-2012 by Ngoumdoun (2013) who calculated P = 1840 mm, R = 1640 mm,
307 ρ = 0.88 and AET = 220 mm (see Supplementary Material, Sect. 4).

308

309 **3.4 Dedicated short-term multi-scale instrumentation (03/2017-02/2018)**

310 In order to complete historical data, we undertook dense spatial rainfall-runoff instrumentation during one
311 hydrological year (03/2017-02/2018). Eleven daily time step raingauges were installed in order to study the spatial
312 variability of precipitation (Fig. 4a). The choice of limnimetric stations location was determined by the position of
313 the main confluences, by the position of historical limnimetric stations, and the need to measure runoff from basins
314 with different degrees of urbanization (Fig. 4a). This instrumentation provides six additional experimental donors
315 (noted D_I) with different ranges of heterogeneities in terms of area, land-use, topography and soil (Table 1). The
316 limnimetric station D_{I1} is located downstream the dam and enables to measure the outflow from the reservoir at
317 100 ± 25 mm.yr^{-1}. The lack of measurements of the outflow value until 2017-2018 makes this results the first
318 assessment of the dam impact on Mefou water budget. The donor D_{I4} corresponds to the intermediate basin between
319 D_{I3} and $D_{I2.}$ Table 1 presents their characteristics: area between 21 and 120 km², P between 1620 and 1715 mm, R
320 between 712 and 1250 mm, ρ between 0.40 and 0.76 and AET between 405 and 908 mm. Annual precipitation on
321 these donors D_I are of the same order as for historical donors D_H while runoff and runoff coefficients are generally
322 higher for catchments with higher urbanization rate.

323

324 **3.5 Main characteristics of the donor catchments**

325 The Mefou catchment originally covers by dense tropical forest includes the most part of the city of Yaoundé.
326 The urban area started growing since 1960 (1 % of the total basin area) to currently reach about 30-35 % of the
327 basin area with an impervious area estimated to 15 %. The forest cover has vanished of more than 50 % since 1980
328 with a huge conversion of the primary forest into secondary and degraded forests. Nowadays, the forests cover
329 about 40 % of the Mefou at Nsimalen. The various sources cited in Sect. 3.2 showed a growth of agricultural areas
330 around the urban area of Yaoundé, with cropland and grassland covers around 30 % of the catchment area in 2015.
331 The catchment can be considered as peri-urban due to the noticeable urbanization and the development of
332 agricultural activities observed in lowlands and outskirts. However, the south-west part and the area drained by
333 the Mopfou dam in upstream remain slightly affected by urbanization.

334 Combining historical studies and dedicated short-term instrumentation 2017-2018, we have 12 donor
335 catchments, 6 from historical studies (D_H) and 6 from the instrumentation (D_I) presenting various topographic, soil
336 and land-use characteristics; the area ranges between 21 and 235 km², P ranges between 1620 to 1930 mm, R
337 between 390 and 1340 mm, ρ between 0.22 and 0.77 and AET between 400 mm to 1400 mm. S_I varies from 6.7 %
338 to 13.5 %, HS varies from 0 to 44 % and U varies from 0 to 83 % over donor catchments of the study area. We
339 observe that ρ can vary widely for the same catchment function of the land-use: e.g. from 0.33-0.4 for D_{H1} (U =
340 5 %) and D_{H2} to 0.77 for D_{H3} (U > 75 %). All the observed data on the study site are analysed to understand

hydrological processes of the catchments faced to land-use changes in order to identify rules defining the hydrological index *I* on donors and apply it on targets for the period 1930-2017.

4 Precipitation

The model needs as input the precipitation *P* which has to be calculated on both donor and target catchments (Fig. 4). For donors, precipitation information are well documented in corresponding studies or issue of dedicated short-term instrumentation (Table 1). For targets, we used the long-term historical raingauges and the spatially short-term information (1968-1969 from SNEC (1969), and 2017-2018 from the short-term instrumentation) to construct historical precipitation database for each target.

4.1 Temporal variability of precipitation

First, we study long-term precipitation trends (1930-2015) over the Mefou catchment from historical raingauges P_1 and P_2. The average precipitation is 1580 mm (P_m) and the minimal and maximal annual precipitation are respectively P_n = 1050 mm and P_x = 2200 mm. Values of P_n and P_x set the limit of availability of the developed model for the study catchment. Fig. 5a shows no significant trends of annual precipitation over the period, but we observe a succession of humid (1960-1970, 1980-1990, and 2006-2013) and dry (1935-1950, 1970-1980, and 1990-2000) periods. At the seasonal scale we observe some changes in amount of precipitation: i) no change during the first wet season (March to June) (Fig. 5b); ii) during the first dry season (July and August), increase of the mean precipitation from 100 to 220 mm (+120 %) on the period 1930 to 2015 (Fig. 5c); iii) during the second wet season (September to November) slight increase from 700 to 760 mm (+9 % ; Fig. 5d); iv) during the second dry season (December to February) decrease from 110 to 80 mm (-28 %; Fig. 5e). This historical precipitation database is used to construct the database precipitation for target catchments. Results shows also that there is no a clear changes on annual precipitation between 1930 and 2015, and consequently the trend of annual runoff coefficient increase can be related mainly to catchment change and particularly to the increase of urbanized areas.

4.2 Spatial variability of precipitation

Second, we study the spatial distribution of annual precipitation over the Mefou catchment.

Figures 6a and 6b show the mean annual precipitation for respectively the hydrologic years 1968-1969 (SNEC, 1969) and 2017-2018 (dedicated short-term instrumentation), the only historical years with available dense spatially measured precipitation.

For 1968-1969, *P* varies over the Mefou catchment between 1400 mm to 2000 mm with an average of 1780 mm. For 2017-2018, *P* varies between 1400 and 2100 mm with an average of 1640 mm. The hydrological year

2017-2018 seems quite representative of an average year in terms of annual precipitation (P_m = 1580 mm). The annual precipitation observed at P_1 is about 1730 mm for the same period with a difference of +6 % with average precipitation P. The rain-gauge P_1 seems quite representative of the average value for the Mefou catchment.

On both Figs. 6a and 6b, we observe that the highest annual precipitation values are located in the north-west part of the basin, corresponding to the zone with highest elevations. The east and south parts, corresponding to the flattest and lowest elevation parts of the basin are characterized by lower P.

Due to the lack of spatial information for the historical period, a precipitation weight w_{Ti} is assigned to a target catchment T_i such as:

$$P_{Ti} = w_{Ti} . P \ , \quad (12)$$

where P is the mean annual precipitation on the Mefou catchment from the historical database and P_{Ti} the mean annual precipitation on T_i. The term $w_{Ti} = P_{Ti}/P$ can be both calculated using historical data (Figs. 6a and 6c) and the instrumentation 2017-2018 (Figs. 6b and 6d). For both cases, we obtain comparable and retain $w_{T1} = w_{T3} = w_{T5} = w_{T6} = w_{T7} = 1$ for respectively T_1, T_3, T_4, T_5, T_6 and T_7; $w_{T2} = 1.05$ for T_2 is slightly high due to the high values of P; $w_{T4} = w_{T8} = 0.95$ for T_4 and T_8.

4.3 Relationship between annual runoff coefficient and precipitation

Third we study the relationship between the annual runoff coefficient ρ and P for three stations in nearly-steady land-use states (Fig. 7): the Mefou at Nsimalen on the period 1964-1984 with a low impact of land-use evolution in comparison to the period 1984-2015, the Mefou at Etoa natural forested basin on the period 1967-1983, and the semi-urbanized Mfoundi on the period 1969-1971. Both the Mefou at Etoa and Mfoundi are sub-catchments of the Mefou at Nsimalen. For the Mefou at Nsimalen, we adjusted a linear relationship between ρ and P; ρ increases from $\rho_{n,P} = 0.2$ corresponding to P_n = 1050 mm to $\rho_{x,P} = 0.35$ corresponding to P_x = 200 mm; this gives $\beta_1 = \rho_{x,P} - \rho_{n,P} = 0.15$. For the Mefou at Etoa, $\rho = 0.15$ for P = 1330 mm and $\rho = 0.30$ for P = 2200 mm; both values of ρ for the Mefou at Etoa are inferior than those observed on the Mefou at Nsimalen for similar values of precipitation, showing the impact of land-use with low annual runoff coefficient on natural basins. For the Mfoundi, $\rho = 0.33$ for P = 1640 mm and $\rho = 0.40$ for P = 1930 mm; both values of ρ for the Mfoundi are superior than those observed on the Mefou at Nsimalen for similar values of precipitation, showing the impact of land-use with high annual runoff coefficient on semi-urbanized basins. In summary, we obtain approximately similar values of β_1 = 0.15 on the Mefou at Nsimalen (1964-1984), but also on the natural Etoa catchment (1967-1983) and on the in-urbanization Mfoundi upstream catchment (1969-1970). These three catchments have three different values of the hydrological index I, but with I considered constant on the presented periods.

Hydrol. Earth Syst. Sci. Discuss., https://doi.org/10.5194/hess-2019-116
Manuscript under review for journal Hydrol. Earth Syst. Sci.
Discussion started: 2 May 2019

5 The hydrological index I

This section analyses the hydrological and physiographic data in order to define the rules for constructing the hydrological index I calculated as a linear combination of three components:

$$I = \omega_T C_T + \omega_S C_S + \omega_{LC} C_{LC} \ , \quad (13)$$

where C_T is the topography component, C_S the soil component, C_{LC} the land-use component, ω_T the weight of C_T, ω_S the weight of C_S, and ω_{LC} the weight of C_{LC}.

5.1 The components C_T, C_S and C_{LC}

Heterogeneities of topography, soil condition and land-use variability in space and time observed on the study area (Sect. 3) lead us to propose classification rules to highlight the main features of catchments and to define the three components C_T, C_S, and C_{LC} of the hydrological index I using cartographical data. All three components range between 0 and 1; when any of the terms (C_T, C_S and C_{LC}) increase, ρ increases. The topography (C_T) and soil condition (C_S) are considered stable over the time contrary to land-use (C_{LC}) faced to major changes.

For topography C_T, the slope index S_I of Roche (Roche, 1963) is calculated for donors (Table 1) and targets from SRTM (2014). We define: $C_T = 0$ for $S_I < 7$ %; $C_T = 0.5$ for $7\ \% \leq S_I \leq 12$ %; $C_T = 1$ for $S_I > 12$ %.

For soil condition C_S, the lack of accurate soil maps over the catchment constrains us to define indirectly soil condition heterogeneities over the catchment. Historical studies of soil characteristics (Bachelier, 1959; Pellier, 1969; Humbel and Pellier, 1969) are used to define soil classes depending on the altitude and the slope derived from the SRTM 2014. For that, we calculate the area of lowlands (altitude < 730 m) with low slopes (< 7 %) corresponding to hydromorphic yellow soil characterized by lower rate in clay and higher surface permeability. The proportion of hydromorphic soil (HS) on each catchment is used to estimate the classes of C_S (see for donors Table 1, and for targets: $C_S = 0$ for $HS > 15$ %; $C_S = 0.5$ for $2\ \% \leq HS \leq 15$ %; $C_S = 1$ for $HS < 2$ %.

For land-use component C_{LC}, historical references and global products (summarized in Table 2) are used to characterize land-use of donors and the evolution of target land-use over past-period with available data (1930, 1950, 1980, 2000, and 2017) and future scenario (2030). In order to integrate the main land-use signature, we define six classes for C_{LC} according to urban area proportion of (U; see for donors Table 1, and for targets the Supplementary Material, Table S3): $C_{LC} = 0$ for $U < 1$ %; $C_{LC} = 0.2$ for $1 < U < 5$ %; $C_{LC} = 0.4$ for $5 < U < 20$ %; $C_{LC} = 0.6$ for $20 < U < 50$ %; $C_{LC} = 0.8$ for $50 < U < 70$ %; $C_{LC} = 1$ for $U > 70$ %. Different trends of land-use changes are observed for the 8 target sub-catchments (Fig. 8). From 1930 to 1950, the whole main catchment is considered to be mostly cover by originally forest ($C_{LC} = 0$ for all the targets). Development of urbanization impacted first the Mfoundi sub-catchments from 1960 to 1980 (T_5, T_6 and T_7) especially T_5. Nowadays, these sub-catchments reach a maximum of urbanization for T_5 and T_6 ($C_{LC} = 1$). T_2 and T_8 faced to major changes since 1980 with intensification since 2000. Nowadays, the urbanization process do not get the entire area of these catchments. The urbanization continue and will be amplified in these surrounding areas due to the lack of space in the most urbanized part of Yaoundé (T_5, T_6 and T_7). T_1, T_3 and T_4 are the last sub-catchments impacted by urbanization; a high proportion of these catchments have forest or wetland covers. We propose a fictive but plausible scenario of land-use for 2030, regarding to the current expansion of the urban area and the perspective of future population

Hydrol. Earth Syst. Sci. Discuss., https://doi.org/10.5194/hess-2019-116
Manuscript under review for journal Hydrol. Earth Syst. Sci.
Discussion started: 2 May 2019

estimation for Yaoundé (from 3.6 million in 2017 to 6.7 million in 2035; UNDESA, 2017). We suppose a high development of urbanization for T_2 and T_8 (C_{LC} from 0.6 in 2017 to 0.8 in 2030) and in a lesser extent a development of urbanization over the south part of the basin (T_4 with C_{LC} from 0 in 2017 to 0.4 in 2030). Values of C_T, C_S and C_{LC} are presented for donors in Table 3 and for targets in Table 4.

5.2 Relationship between annual runoff ρ and C_T, C_S and C_{LC} for donors

D_{H4}, D_{H5} and D_{H6} correspond to forested areas ($C_{LC} = 0$) whereas D_{I5} and D_{H3} have high rates of urbanization ($C_{LC} = 1$, Table 3). For these basins, precipitation presents a low range of variation between 1645 and 1810 mm. D_{H4}, D_{H5} and D_{H6} present low values of annual runoff coefficient with ρ varying from 0.22 to 0.25. D_{I5} and D_{H3} present very high values of runoff with $\rho = 0.76$ and 0.77. For catchments with intermediate levels of urbanization (D_{I2}, D_{I3}, D_{I4}, D_{I6}, D_{H1}, D_{H2}), runoff ranges between those observed in the two previous cases with ρ ranging between 0.33 and 0.54.

Analysis of ρ for donors D_{I2} and D_{I6} presenting the same value of C_{LC} (0.6) but extreme values of C_T and C_S (D_{I2} is located in the hilly part of the Mefou catchment whereas D_{I6} present high portion of lowlands) enables to quantify the impact of C_S and C_T on ρ. For the period September-December, D_{I6} presents runoff coefficient of 0.40 which is significantly lower than the value of 0.53 observed for D_{I2} on the same period. Differences observed are quite clear in term of runoff with for D_{I4} runoff value up to 160 mm in October against 95 mm for D_{I6} (see Supplementary Material, Sect. 5).

These results show the significant impact of land-use conditions on runoff, but topography and soil condition could explain complex hydrological responses. Consequently when calculating the index I, we will give a higher weight to the component C_{LC} in comparison to C_T and C_S.

5.3 The weights ω_T, ω_S and ω_{LC}

From data analysis (Sect. 5.2), we showed that the impact of land-use change on runoff is higher than the impact of soil and topography. Consequently, we affect higher weight for ω_{LC}, with $\omega_{LC} > \omega_T$ *and* $\omega_{LC} > \omega_S$. Figure 9 shows an example of the relationship between annual runoff of donors ρ and hydrological index for donors I for $\omega_{LC} = 7/9$, $\omega_T = 1/9$ and $\omega_S = 1/9$. We observe a simple linear empirical relationship to estimate ρ_D :

$$\rho_D = aI + b \quad (14)$$

with $r^2 = 0.96$. We conduct a sensitivity analysis of the regression on the adjusted parameters a and b for four sets of parameters ω_{LC}, ω_T and ω_S : i) $\omega_T = 1/5$, $\omega_S = 1/5$ and ω_{LC},= 3/5; ii) $\omega_T = 1/7$ $\omega_S = 1/7$ and ω_{LC},= 5/7; iii), $\omega_T = 1/9$, $\omega_S = 1/9$ and ω_{LC}= 7/9; iv) $\omega_T = 1/12$, $\omega_S = 1/12$ $\omega_{LC} = 10/12$. We obtain very good correlation coefficient of the four linear regressions ranging between 0.83 (case i) and 0.98 (case iv). The parameter a ranges between 0.66 and 0.83, and the parameter b between 0.10 and 0.19 (note that for $I = 0$ we have $\rho = b$). For $I = 1$, we have $\rho = a$

Hydrol. Earth Syst. Sci. Discuss., https://doi.org/10.5194/hess-2019-116
Manuscript under review for journal Hydrol. Earth Syst. Sci.
Discussion started: 2 May 2019

478 + b which varies between 0.80 and 0.84. Around a mean value of I = 0.5, all four configurations give ρ = 0.51 (See
479 Supplementary Material, Sect.6).

480 For the configurations ii, iii and iv, we have r^2 = 0.96 +/- 0.02. In the following, we retain the intermediate
481 set ω_T = 1/9, ω_S = 1/9 and ω_{LC}= 7/9 (corresponding regression presented in Fig.9). Table 3 presents the values of
482 I for donors and Fig. 10 gives the temporal evolution of I from 1930 until now for targets. Note that in 2017, the
483 values of I are particularly high for the target catchments T_5, T_6 and T_7 on the Mfoundi basin due to high
484 urbanization. In contrast, some target catchments such as T_1 and T_4 are or not impacted nowadays by urbanization
485 and presents very low values of I. Finally, the target catchments T_2, T_3, and T_8 are currently faced to the most
486 important land-use change and have intermediate values of I.

487

488 **5.4 Introducing *I* in the model structure**

489 In the following, we choose a simple linear relationship between I and ρ (Eq. 14; Fig. 9) which leads that the
490 value of β_1 is constant and similar for all values of I.

491 We observe that the impact of land-use change (represented by I) on annual runoff (β_2) is higher than the
492 impact of precipitation change (β_1), with β_1 = *0.15* (Fig. 7), β_2 = 0.60 (Fig. 9) and $\beta_1 << \beta_2$. We consider a
493 reference precipitation $P_R = \frac{P_x+P_n}{2}$, and let ρ_D be the runoff coefficient calculated by the linear regression adjusted
494 from donors under precipitation near of P_R (1625 mm). Then ρ is calculated as the sum of ρ_D and a factor G taking
495 into account the impact of precipitation:

496 $$\rho = \rho_D + G \,, \tag{15}$$

497 with

498 $$G = \frac{\beta_1}{(P_x - P_n)} \left[P - \frac{P_x+P_n}{2} \right] . \tag{16}$$

499 For a given value of I (Fig. 9): for $P = P_n$, we have $G = -\beta_1/2$ and consequently $= \rho_D - \frac{\beta_1}{2} = \rho_{n,P}$; for
500 $P = P_x$, we have $G = \beta_1/2$ and consequently $\rho = \rho_D + \frac{\beta_1}{2} = \rho_{x,P}$.

501 Introducing Eq. (14) and (16) into Eq. (15), we obtain very simple second order polynomial relationship
502 between R and P (Eq. 17 similar to Eq. 1) and a linear relationship between ρ and P (Eq. 18 similar to Eq. 2), and

503 $$R = AP^2 + BP \,, \tag{17}$$

504 $$\rho = AP + B \,, \tag{18}$$

505 with $A = \frac{\beta_1}{P_x - P_n}$ and $B = aI + b - \frac{\beta_1 (P_x+P_n)}{2(P_x-P_n)}$. (19)

506 In summary, the model needs the precipitation P as input and the three parameters a, b and β_1 characterizing
507 the relationship between ρ and I. These three parameters can be calibrated using data from donor catchments.

6 Applications

The model presented in Sect. 2 is function of precipitation P and the hydrological index I. Precipitation was calculated on the target sub-catchments using historical precipitation dataset and the relationships established in Sect. 4. The hydrological index I is defined in Sect. 5 and presented in Fig. 10 for target catchments for the period 1930 - 2030.

First a sensitivity analysis was conducted and the calibrated parameters a, b of the model are discussed (Sect. 6.1). Then two applications were conducted on the Mefou at Nsimalen subdivided into eight target sub-catchments (Fig. 4.b) in order:

- to study the spatial hydrological functioning of the basin on eight target sub-catchments and calculate the water balance during the short instrumentation period 2017-2018 (Sect. 6.2).
- to reconstruct the hydrograph at the Mefou at Nsimalen and on the eight sub-catchments for the historical period 1930-2017 and to simulate the impact of future scenarios of land use and urbanization (Sect. 6.3).

6.1 Sensitivity analysis, calibration, validation and model comparison

Applications were conducted on the period 1930-2017, using precipitation data on P_1 and P_2, to reconstruct annual runoff for all eight target sub-catchments and the whole Mefou catchment at Nsimalen. Predictions for the impact assessment of future land-use scenario on annual runoff were then also made. In the application, we distinguish two cases, before and after the dam construction (1970). Before 1970, the catchment T_1 (controlled area of the dam location) is considered as other catchments (R depends of I and P). After 1970, the simulated R of T_1 corresponds to the proportion of precipitation discharged measured during the short-term instrumented period (ρ = 0.05 to 0.15; see Table 1 for D_{I1} and Sect. 3.4).

From data analysis in Sect. 4.3 (Fig. 7), we retain β_1 = 0.15. We run a sensitivity analysis on the remaining two parameters a and b (adjusted from the regression $\rho_D = aI + b$ with I calculated using Eq.13 with ω_T = 1/9 and ω_S = 1/9, ω_{LC} = 7/9) for different sets of donor catchments. We run the model for n = 6, 8, 9 and 10 donors (see Table 1 and Sect. 3.3 and 3.4). In each run, we select randomly 30 sets of n donors, and in order to have a wide range of variation of I, we add a constrain that for at least one point we have I < 0.3 and for at least one point we have I > 0.7. The model output is given by Eq. 1 to 6 at the Mefou at Nsimalen, and the model is evaluated using the three criteria $RMSE$ (Eq. 8) and r^2 (Eq. 9) and $\bar{E}$ (Eq. 11) for the 29 observed years (see Sect. 3.3). For n = 6, 8, 9 or the 10 donors, we observe a low impact of the number of donors on the calibrated parameters (a and b) and the three performance criteria with a = 0.68 +/- 0.02, b = 0.12+/- 0.01, $RMSE$ = 101+/-1 mm, r^2 = 0.66, and $\bar{E}$ = 15 % (see Supplementary Material, Sect. 6). The low variability of the average of parameters a and b from n = 8 lead us to select 8 donors by keeping the last two donors for validation.

In order to get a model adapted to various states of urbanization, the calibration and validation dataset at the Mefou catchment scale should include periods of low and high urbanization rate. Observed annual runoff at the Mefou at Nsimalen are used in alternate years for calibration (15 years) and validation (14 years). From the sensitivity analysis, we calibrate a and b, choosing the set of 8 from 10 donors giving the lowest values of $RMSE$

on the 15 years calibrated period. We use the 9 donors D_{H2}, D_{H3}, D_{H4}, D_{H6}, D_{I2}, D_{I3}, D_{I4}, D_{I5} and D_{I6}. We obtain a = 0.74; b = 0.12 with performance criteria *RMSE* = 70 mm, r^2 = 0.79 and $\bar{E}$ = 11 %. Figure 9 presents the linear regression for the calibrated parameters and Fig. 11 shows the abacus $\rho = g(P,I)$ for these parameters. In the abacus, we plotted the donor catchments by specifying the corresponding estimation of I in parenthesis to compare with the model. We also plotted the points of Etoa for the period 1967-1983 characterized by a stationarity value of I (0.11) but with a wide range of P (1320 to 2150 mm).

The validation is made at two levels. First, the two remaining donor catchments D_{H3} and D_{I2} are used to validate; we obtain $E_{D_{H3}}$ = +8 % (+105 mm) and $E_{D_{I3}}$ = +12 % (+110 mm). Second, at the Mefou at Nsimalen for the remaining 14 years; we obtain *RMSE* = 123 mm, r^2 = 0.60, and $\bar{E}$ = 18 %.

The semi-distributed model results were also compared to the stationary lumped annual runoff model *GR1A* (Mouelhi, 2003) using the same calibration and validation procedure. *GR1A* is used to compare with a stationary approach of the catchment characteristics. Results are shown on Fig. 12 with performance for *GR1A* significantly lower with *RMSE* = 126 mm, r^2 = 0.43 and $\bar{E}$ =19 % for calibration and *RMSE* = 128 mm, r^2 = 0.42 and $\bar{E}$ = 22 % for validation over the both same periods at Mefou catchment scale. As the *GR1A* was calibrated using alternate years on the whole period, we observe that *GR1A* slightly overestimate the runoff for the period 1963-1980 (with low impact of urbanization), and underestimates runoff for the period 2011-2017 (with high impacts of urbanization)

6.2 Annual water balance on the instrumented period 2017-2018

The rainfall-runoff data from the short-term instrumentation 2017-2018 enables to measure the contribution of the catchments T_1, T_2, T_3 and T_6 of the Mefou catchment at Nsimalen. However, the target sub-catchments T_4, T_5, T_7 and T_8 were not gauged. Table 5 gives the values of P, R, AET, ρ and the contribution of each sub-catchment K_i, corresponding to runoff volume of sub-catchment V_i divided by the volume at Nsimalen V_O (with $K_i = V_i / V_O$). P ranges between 1580 and 1715 mm, R between 100 and 1325 mm, AET between 320 and 1260 mm, ρ between 0.21 and 0.76 and K between 2.5 to 18.5 %. We can classify the eight target catchments into four categories according to land-use: i) controlled by the dam, T_1; ii) urbanized T_5, T_6 and T_7; iii) peri-urban T_2, T_3 and T_8; iv) natural basins T_4.

The first category concerns the sub-catchment T_1 controlled by the dam. The annual discharge R_1 measured at the outlet of the dam is 100 mm +/-25 mm, corresponding to a contribution K_1 = 2.5 % on the total volume at Nsimalen.

The second category corresponds to sub-catchments firstly faced to urbanization during the study period. We have respectively R_5 = 1230 +/- 125 mm, R_6 = 1130 +/-125 mm and R_7 = 1030 +/- 200 mm. The contribution of T_5, T_6 and T_7 on the total volume at Nsimalen are respectively K_5 = 18.0 %, K_6 = 10.0 % and K_7 = 11.0 %. These three catchments are characterized of by very low AET between 390 and 620 mm and very high ρ between 0.62 and 0.76.

The third category corresponds to peri-urban catchments. Runoff on T_2 (corresponding to D_{I2}) is characterized by R_2 = 915 +/- 90 mm (compared to 1030 mm simulated), ρ_2 = 0.53, AET_2 = 800 mm, and corresponds to 15 % of V_O. T_8, presenting an intermediate land-use characteristics with low slope in the downstream part, has R_8 = 730 +/- 150 mm, ρ_8 = 0.46, AET_8 = 850 mm, and K_8 = 16 %. The main differences between T_2 and T_8 are the topography and the soil characteristics: T_2 is located in the upstream part of the Mefou catchment and presents hilly landscape with steep slopes; T_8 is located in the east side presenting lowland with important wetland area and overflow during wet seasons. These differences explain the lower values of R for T_8 in comparison with T_2. These results are comforted by observed runoff coefficient for the second wet season in 2017: T_2 have an observed runoff coefficient of 0.53 compared to 0.40 for T_8 despite a similar urbanization rate (40 % for T_8 and 46 % for T_2). In the same category, T_3 (D_{I4}) presenting a most natural land-use (10 % of urbanized area) than T_2 and T_8, is characterized by R_3 = 715 +/-75 mm (compared to 700 mm simulated), ρ_3 = 0.43, AET_3 = 905 mm, and K_3 = 18.5 %.

For the fourth category, T_4 is not impacted by urbanization (U < 1%). T_4 is located downstream with low slope, with soil condition and topography favouring overflow, infiltration and evaporation. T_4 presents the lowest R_4 = 370 +/- 50 mm, ρ_4 = 0.24, AET_4 = 1290 mm, and K_4 = 9 %.

For the Mefou at Nsimalen, we obtain by aggregation of the eight sub-catchments: R_O = 660 +/- 65 mm (compared to 645 mm measured at the outlet), ρ_O= 0.41 and AET_O = 990 mm. These values are very near from observed data with annual runoff measured of 645 mm.

These results on the eight target sub-catchments are compared to other studies in the Nyong basin (see Supplementary Material, Sect. 4) on natural basins (Maréchal et al., 2011; Olivry, 1979; Lefèvre, 1966) and on one urbanized basin of the Nyong basin. These studies led to comparable results of ρ with ρ = 0.24 +/- 0.06 on natural basins, and ρ = 0.88 on the urbanized of Odza (Ngoumdoum, 2013) on Nyong basin.

6.3 Reconstruction of historical runoff and prediction for scenarios of land-use

The past-period 1930-2017 simulated for targets and at Nsimalen are presented in Fig. 12. The grey envelope curve represents the estimation of runoff uncertainties due to annual precipitation (+/- 10 %) and hydrological index (+/- 15 %). Except for T_4 (downstream part of Mefou catchment) and T_1 (area controlled by the dam), all the target sub-catchments present an increasing trend of runoff in earlier or later date. In a context of no annual precipitation trends over the period 1930-2017, the urbanization development and forestry retreat for six of the eight targets result in clear increasing of R. We notice that the impact on runoff is until now lesser for T_3 and T_8. In order to quantify impacts of land-use changes, we calculated mean values $\bar{P}$, $\bar{R}$ and $\bar{\rho}$, 5th percentile Q_5 and 95th percentile Q_{95} for one past period (1950-1980) and one recent period (1987-2017) (see Table 6). The mean precipitation over the first period is about 75 mm higher (+ 5%) than for the second period with a similar standard deviation (200 mm). Excluding T_1, controlled by the dam, we obtained on the period 1950-1980 $\bar{R}$ between 315 and 764 mm, $\bar{\rho}$ between 0.20 and 0.47, Q_5 between 200 and 503 mm and Q_{95} between 502 and 1108 mm. On the

period 1987-2017, $\bar{R}$ varies between 297 and 1104 mm, $\bar{\rho}$ between 0.19 to 0.70, Q_5 between 150 and 690 mm and Q_{95} between 508 and 1627 mm.

For the second category (T_5, T_6, T_7), an increasing trend of R is observed very early among the whole period for T_5 and T_6 which are nowadays the most urbanized target of the Mefou catchment following by T_7. Between the two periods (1950-1980) and (1987-2017), $\bar{R}$ increases from 45 % for T_5 to 79 % for T_6, $\bar{\rho}$ increases between 50 % for T_5 to 85 % for T_6. Q_5 increases of 37 % for T_5 to 74 % for T_7 and Q_{95} increases of 47 % for T_5 to 82 % for T_6.

For the third category (T_2, T_3, and T_8), classified as peri-urban catchments, sub-catchments are characterized by an increasing R more delayed compared to catchments of the first category. Current changes are deeply modifying these catchments for the last decade and the urbanization processes will be certainly higher than on other sub-catchments in the near-future due to the current extension of the urban area. Between the two periods, $\bar{R}$ increases of 25 % for T_3 to 62 % for T_8. Q_5 increases of 30 % for T_2 and T_8 but decreases from of 26 % for T_3 whereas the Q_{95} increases for the three catchments, from 48 % for T_3 to 69 % for T_8. Land-use changes were significant only since 2000 for T_3, and impact on R is moderate compared to the two other catchments.

For the fourth category (T_4), T_4 was not impacted by urbanisation, $\bar{\rho}$ is unchanged (0.20) and differences of $\bar{R}$ are only drived by $\bar{P}$ difference of -5% (from 1625 mm to 1550 mm) and impact mainly low flows (-26 % for Q_5). No major changes were observed in this area until nowadays, but in development projects and urban area extension will certainly impact T_4 in near-future.

At the Mefou scale and for the same two periods, we observe an increase of $\bar{R}$ of 27% (from 409 to 518 mm), an increase of $\bar{\rho}$ of 31 % (from 0.25 to 0.33), an increase of Q_{95} of 29% (from 650 to 840 mm) and nearly no changes for Q_5 (from 280 mm to 273 mm). The impact of land-use changes is clear on annual runoff but driest years are much less impacted than wettest years.

In order to quantify only the impact of land-use changes on annual runoff, we applied a constant precipitation of 1580 mm (mean precipitation over the period) for the period 1930-2017 (Fig. 13). Until 1980, the impact of land-use changes seems quite limited, with an increase of 110 mm of R (+ 30%). However, between 1980 and 2017, the increase of R and ρ under the same precipitation condition seems quite relevant with an increase of 53% (from 455 to 700 mm and from 0.29 to 0.44). These hydrological changes are associated with a huge increasing of urban areas from 38 km² over the whole catchment to 130 km² over the same period.

Finally, the model was applied to simulate the impact of scenarios of land-use changes corresponding to predictions of I for 2030 (Fig. 10). Results show for P = 1580 mm, R = 840 +/- 150 mm, ρ = 0.53+/- 0.06 (Fig. 13). We observe an increase of R and ρ of 85 % (from 455 to 840 mm and from 0.29 to 0.53) between 1980 and 2030. Even if this scenario is fictive, it is quite reliable due to the dynamic of land-use changes observed these few decades and knowing the most recent projection of population of Yaoundé.

In tropical context, few studies evaluated the impact of land-use conversion from natural to urbanized area. Most of the studies quantified the impact of conversion from forest or shrub cover into cropland (Gessess et al., 2015; Yira et al., 2016) or forest regeneration (Beck et al., 2013).

649 More studies of annual runoff urbanization impacts have been lead in temperate or Mediterranean climate
650 (see Supplementary Material, Sect. 7), Braud et al. (2013) observed a significate increases of quick-flow and
651 decrease of inter-flow and base-flow in urbanization context on the Yzeron catchment (150 km²). Through
652 modelling, Beighley et al. (2003) estimated for Atascadera Creek (P = 610 mm) an increase of R of more than
653 80 mm (+115 %) for 8 % to 38 % of urban area and an increases of R of 150 mm (+215 %) from 8 % to 52 % of
654 urban area.

655

656

657 **7 Conclusion**

658 Urbanization impacts drastically the water cycle, and this phenomenon will intensify in the future for most
659 tropical regions due to huge population growth and rural exodus. These impacts are complex and not yet quantified
660 especially in tropical area presenting sparse hydrological data. This work is part of the theme *Panta Rhei* of the
661 *IAHS*, and aims to study the impact of land-use change, especially due to urbanization, on annual runoff on the
662 tropical mesoscale catchment of the Mefou, Yaoundé, Cameroon.

663 The methodology combines the processing of historical sparse hydrological data and a dedicated short-term
664 instrumentation (2017-2018) in order to get heterogeneous set of catchments in terms of land-use. Data analysis
665 shows that there is no significant trend on annual precipitation for the last 90 years. However, the analysis of
666 historical precipitation/runoff data on different catchments with different land-uses show an increase of the annual
667 runoff coefficient due to urbanization from 22 % on natural basins to 77 % on urbanized basins.

668 A simple semi-distributed annual runoff model was developed taking into account non-stationarity due to
669 land-use changes. The model is based on a similar approach as proposed by Ponce and Shetty (1995) and uses a
670 hydrological index I characterizing soil, topography and land-use. From data analysis on donor catchments,
671 empirical rules were established to calculate I, and the model parameters. The model can be represented by simple
672 abacus giving relationships between the annual precipitation P, the annual runoff R and the hydrological index I.
673 The non-stationarity of the model is characterized by the hydrological index I which is time variable depending
674 on land-use evolution.

675 Applications were first done on target sub-catchments of the Mefou basin in order to calculate the annual
676 water balance for catchments with different land-uses. Results show that that the Mfoundi catchment, integrating
677 the three more urbanized sub-catchments, contributes near to 40 % of the Mefou catchment at Nsimalen despite
678 covering only 23 % of the basin. On the opposite, the natural sub-catchment T_4, not yet impacted by urbanization,
679 contributes to only 9 % but covers 18 % of the Mefou catchment. The second result is the reconstruction of
680 historical annual runoff from 1930-2017 for the Mefou catchment at Nsimalen with satisfying performance in a
681 poorly-gauged context ($RMSE$ = 99 mm; r^2 = 0.68; $\overline{E}$ = 14.5 %) compared to the commonly used stationary annual
682 model (GR1A). The mean values of P, R, ρ, Q_5 and Q_{95} over the two periods of 30 years before and during the
683 urbanized processes show changes at both the sub-catchment scale and the whole Mefou scale: for a decrease of
684 about 50 % of the forest area and an increase from 8 % to 35 % of the urban area between 1980 and nowadays, we
685 observe an increase of 53 % of R (and ρ) for the Mefou catchment at Nsimalen. The Future scenario of land-use

686 proposed leads to an increase of R and ρ of 85 % between 1980 and 2030. The observed and simulated values for
687 heterogeneous land-use characteristics are in line with other studies which observed an increasing of annual runoff
688 for catchment faced to urbanization (Braud et al., 2013; White and Greer, 2006; Barron et al., 2003).

689 The coupled experimental-modelling approach proposed herein opens promising perspectives regarding the
690 evaluation of annual runoff in catchments under changes. Nowadays, development of low cost monitoring sensors
691 and crowdsourced sciences open opportunities to get more easily data to calibrate and validate models. In changing
692 context, the development of coupled non-stationary modelling and dedicated instrumentation can be useful to
693 improve the capability of stakeholders to make predictions of the hydrological dynamics of tropical peri-urban
694 catchments.

695

696

697

698

Data availability. Please contact the first author (Camille Jourdan) for data.

Author contributions. C.J, V.B.E, RM., D.S., and E.S. developed the study framework and prepared the paper structure; C.L. elaborated a first; C.J., A.F., J.B.B., V.B.E., D.S., B.N.G., J.R.N., and S.V.E performed field instrumentation and measurements; A.C, F.C contributed to the interpretation and the discussion of the results; C.J. and R.M. wrote the paper with contributions from all authors.

Supplement. A supplementary material is provided to complete the paper.

Competing interests. The authors declare that they have no conflict of interest.

*Acknowledgements :*We acknowledge the LMI PICASS'EAU and the LMI DYCOFAC of the French National Research Institute for Development (IRD) for their support; Dr J-C Ntonga (IRGM-CRH) for his collaboration ; Jean-Pierre Bricquet, Hélène Mathieu-Subias for technical support in field instrumentation and data collection; Marielle Gosset for the financial support; David Badoga, Moustapha Djangue, Lionel Yossa, Souleyman Abba, Daoud Nsangou and all the students involved in the field schools Hydraride (2016 and 2017) for their contribution; and Nathalie Rouché for historical database information (SIEREM). Authors have a thought for the late Jean-Pierre Bedimo Bedimo for whom it was among his last projects.

Hydrol. Earth Syst. Sci. Discuss., https://doi.org/10.5194/hess-2019-116
Manuscript under review for journal Hydrol. Earth Syst. Sci.
Discussion started: 2 May 2019

719

Figures

720

Hydrol. Earth Syst. Sci. Discuss., https://doi.org/10.5194/hess-2019-116
Manuscript under review for journal Hydrol. Earth Syst. Sci.
Discussion started: 2 May 2019

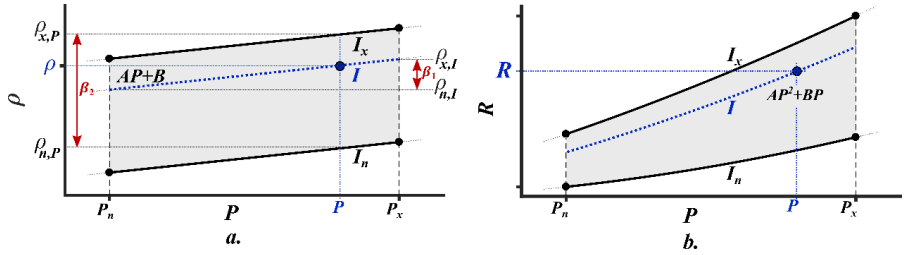

Figure 1. The model general relationships between annual precipitation P, annual runoff R, annual runoff coefficient ρ and the hydrological index I. (a) Relationship between ρ and P with $\rho = AP+B$ for different ranges of I; (b) Relationship between R and P with $R = AP^2+BP$ for different ranges of I. P_n: minimum P; P_x: maximum P; I_n: minimum I; I_x: maximum I. The point in each graph is an example of annual runoff coefficient and annual runoff estimation for a precipitation P and an hydrological index I.

Hydrol. Earth Syst. Sci. Discuss., https://doi.org/10.5194/hess-2019-116
Manuscript under review for journal Hydrol. Earth Syst. Sci.
Discussion started: 2 May 2019

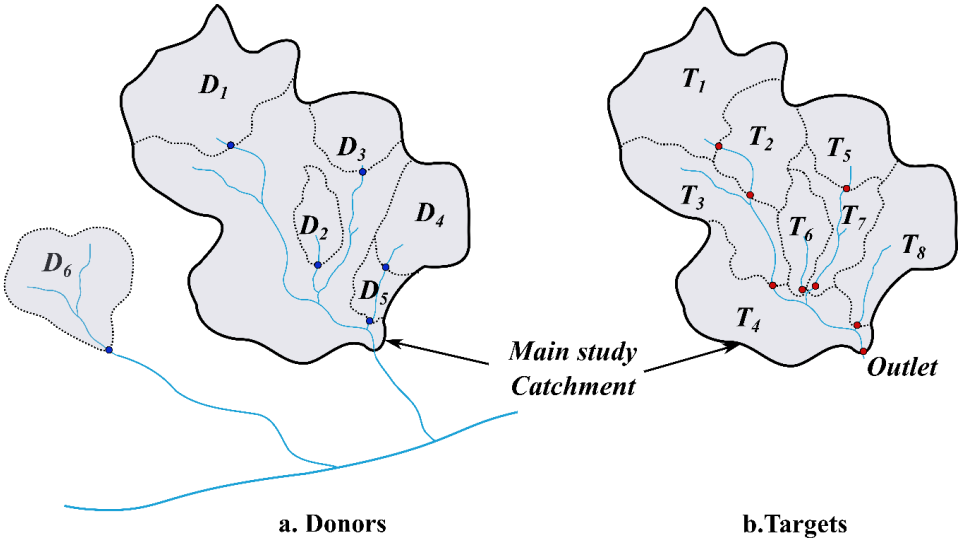

Figure 2. Example of fictive donor (a) and target (b) catchments.

Hydrol. Earth Syst. Sci. Discuss., https://doi.org/10.5194/hess-2019-116
Manuscript under review for journal Hydrol. Earth Syst. Sci.
Discussion started: 2 May 2019

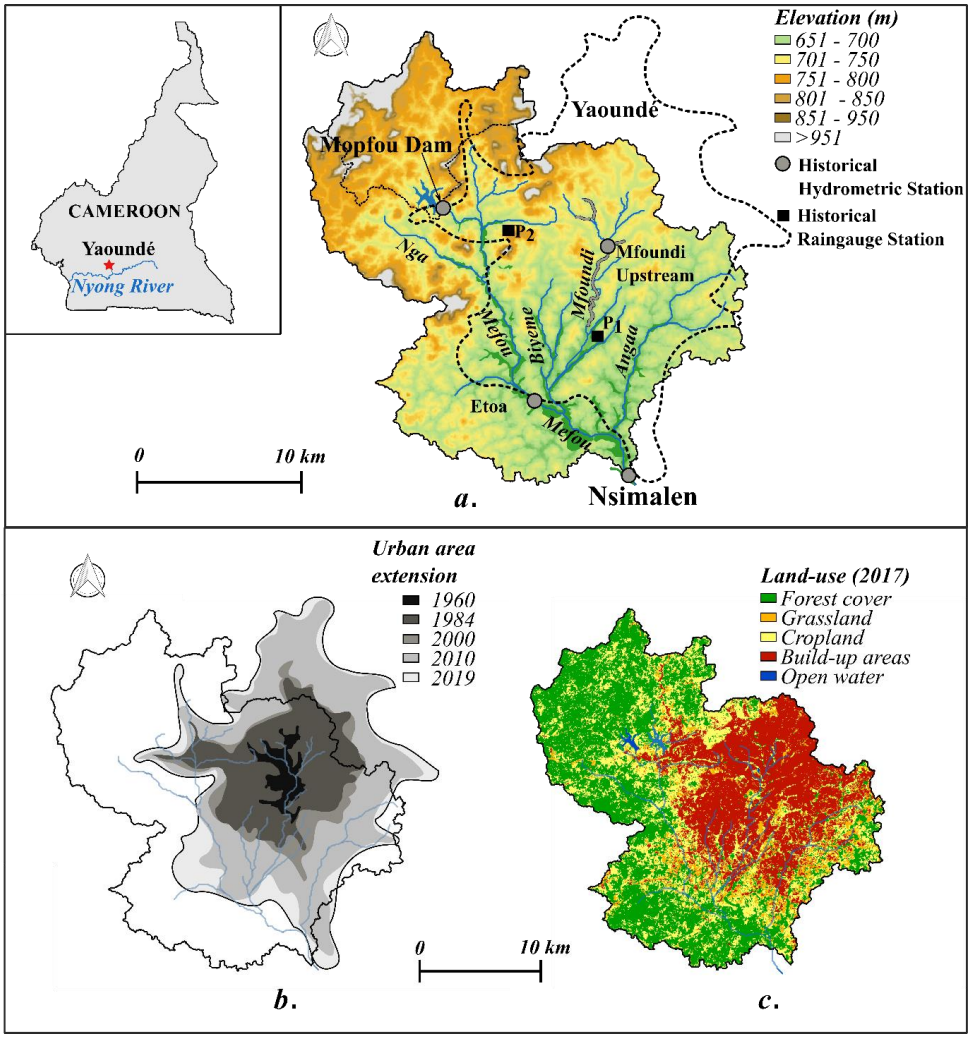

Figure 3. The Mefou catchment at Nsimalen: (a) Location, channel network and topography. (b) Urban areas evolution from 1956 to 2018 from historical photography (Moffo, 2011) and satellite images (Google Earth ®) (c) Land-use extracted from the product Land Cover for Africa of European Space Agency (ESA-LC), based on one year Sentinel-2A observations from December 2015 to December 2016.

Hydrol. Earth Syst. Sci. Discuss., https://doi.org/10.5194/hess-2019-116
Manuscript under review for journal Hydrol. Earth Syst. Sci.
Discussion started: 2 May 2019

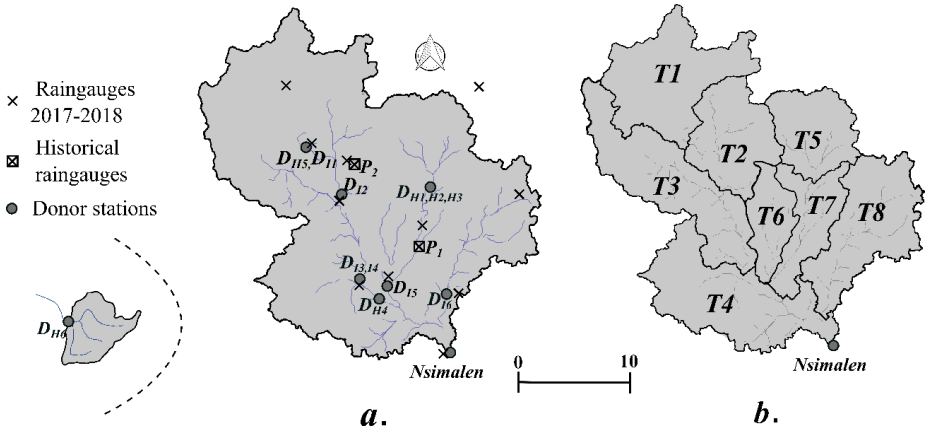

Figure 4. The Mefou catchment: (a) Location of raingauges and limnimetric stations on donor catchments (NB: the donor D_{H6} is located outside of the Mefou basin at 40 km south-west); (b) target catchments.

746

Hydrol. Earth Syst. Sci. Discuss., https://doi.org/10.5194/hess-2019-116
Manuscript under review for journal Hydrol. Earth Syst. Sci.
Discussion started: 2 May 2019

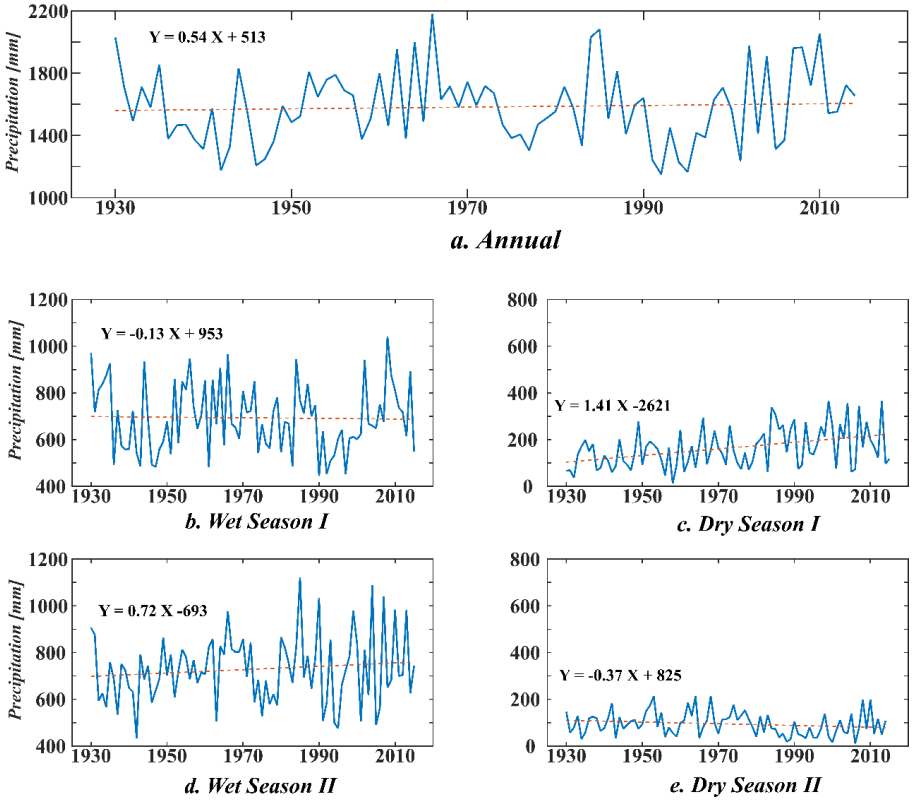

747

748 **Figure 5.** Annual and seasonal precipitation: (a) Annual precipitation from 1930 to 2015 from historical raingauge
749 P_1 (Mvan Airport). (b) Precipitation during the wet season *I* March to June. (c) Precipitation during the dry season
750 *I* July to August. (d) Precipitation during the wet season *II* September to November. (e) Precipitation during dry
751 season *II* December to February.

752

753

Hydrol. Earth Syst. Sci. Discuss., https://doi.org/10.5194/hess-2019-116
Manuscript under review for journal Hydrol. Earth Syst. Sci.
Discussion started: 2 May 2019

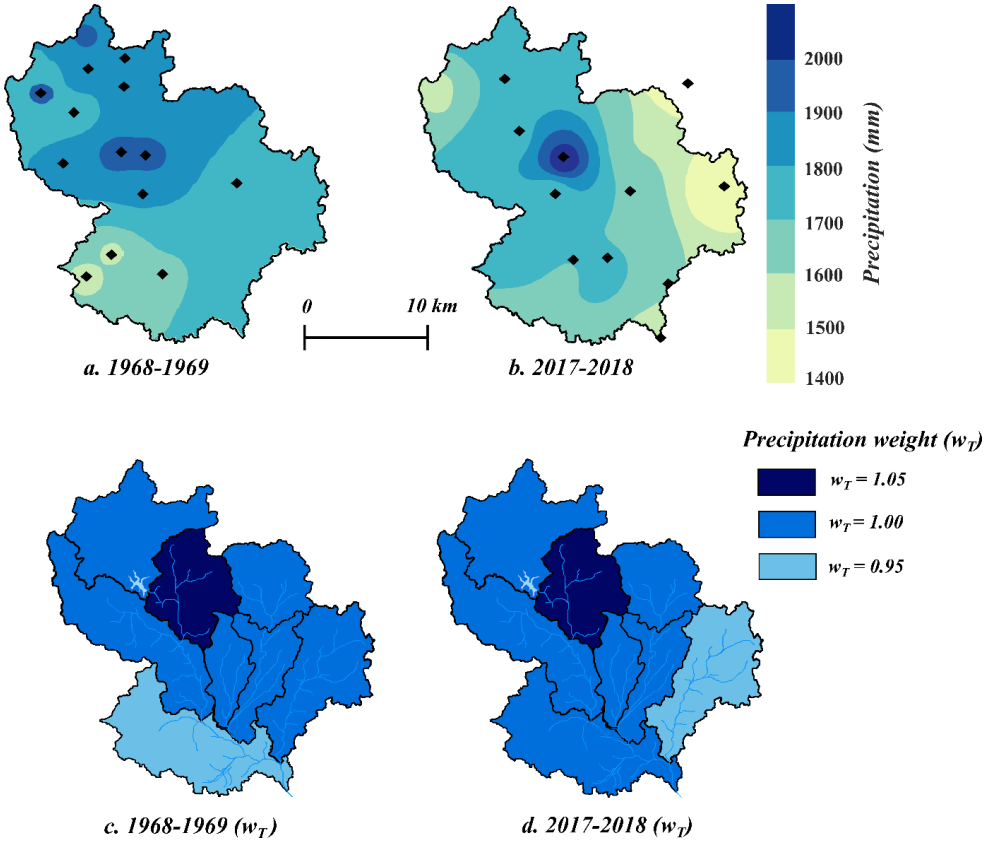

754

755 **Figure 6.** Annual precipitation map on the Mefou catchment: (a) for 1968-1969 (Ikounga, 1978); (b) for the
756 instrumented period (March 2017 to February 2018). Precipitation weights on the 8 target catchments: (c)
757 calculated from (a); (d) calculated from (b).

758

759

Hydrol. Earth Syst. Sci. Discuss., https://doi.org/10.5194/hess-2019-116
Manuscript under review for journal Hydrol. Earth Syst. Sci.
Discussion started: 2 May 2019

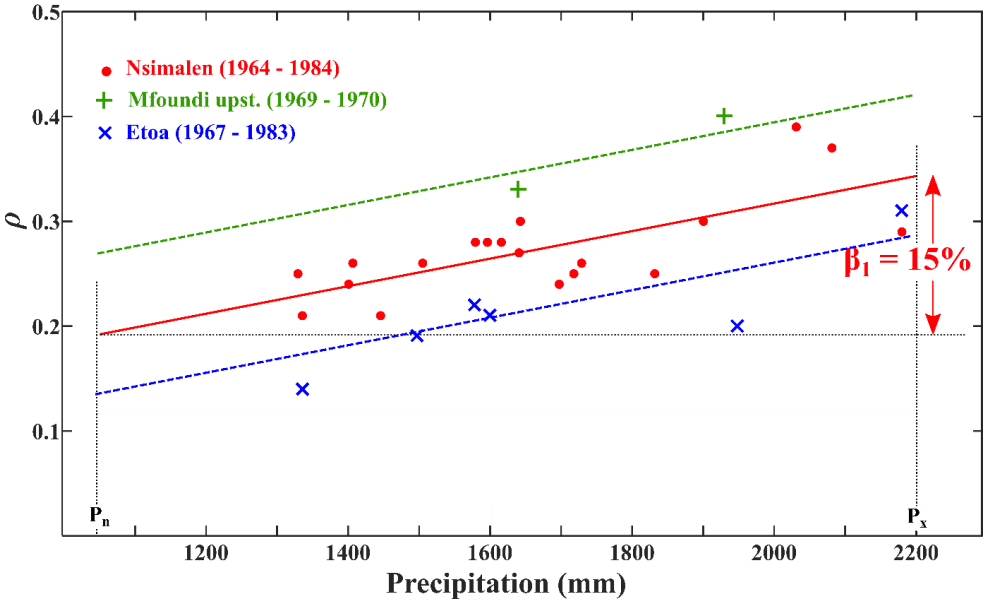

Figure 7. Relationship between the annual runoff coefficient ρ and the annual precipitation P on three stations (Nsimalen, Mfoundi and Etoa; see the location on Fig. 3.a) for periods before 1985 with low impact of urbanization.

Hydrol. Earth Syst. Sci. Discuss., https://doi.org/10.5194/hess-2019-116
Manuscript under review for journal Hydrol. Earth Syst. Sci.
Discussion started: 2 May 2019

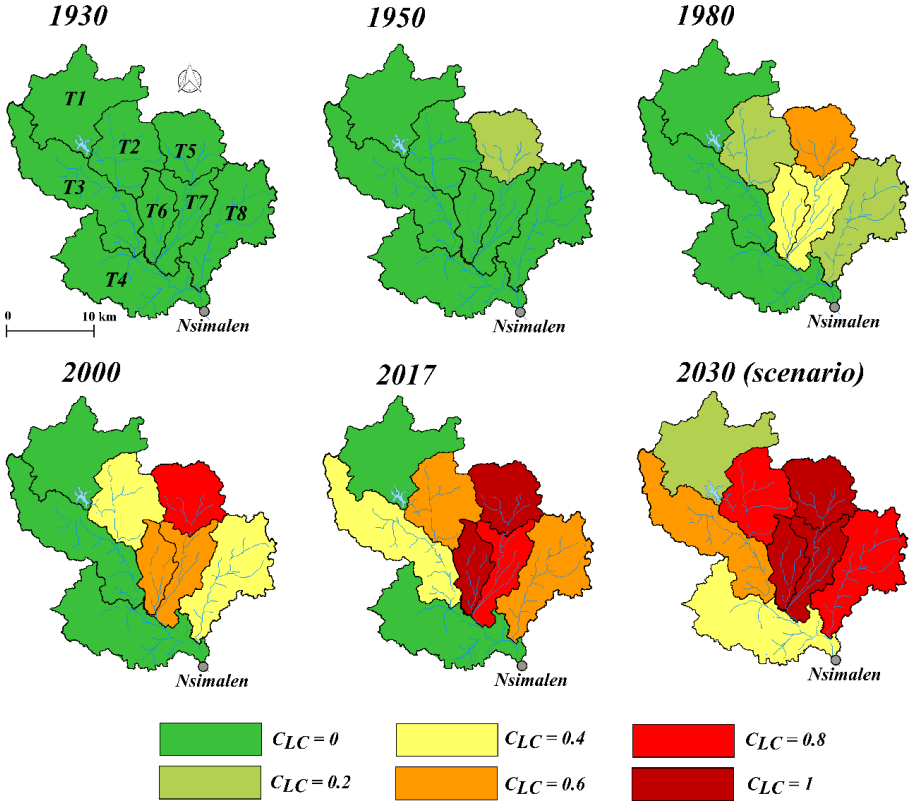

Figure 8. Evolution of the component C_{LC} (see Section 5.1) of the hydrological index I over the target catchments for 1930, 1950, 1980, 2000, 2017 and scenario for 2030 (see references of land-use sources in Table 2).

Hydrol. Earth Syst. Sci. Discuss., https://doi.org/10.5194/hess-2019-116
Manuscript under review for journal Hydrol. Earth Syst. Sci.
Discussion started: 2 May 2019

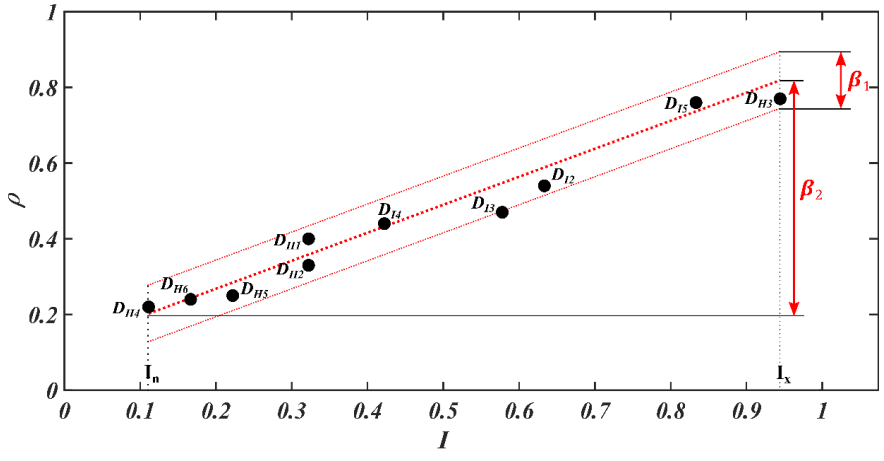

Figure 9. Linear relationship between the hydrological index I and the annual runoff coefficient ρ based on donor catchments (Table 1). The term β_1 represents the variation of ρ for a given value of I and for a large range of precipitation P with $P_n < P < P_x$. The term β_2 represents the variation of ρ for a given value of P and for a large range of I with $I_n < I < I_x$.

Hydrol. Earth Syst. Sci. Discuss., https://doi.org/10.5194/hess-2019-116
Manuscript under review for journal Hydrol. Earth Syst. Sci.
Discussion started: 2 May 2019

Hydrology and Earth System Sciences
Discussions

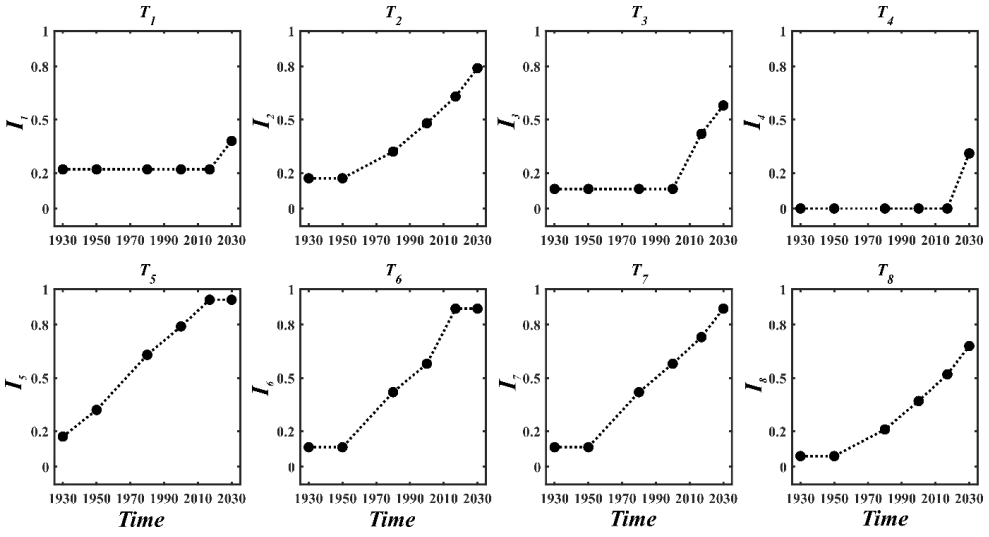

780
781

782 **Figure 10.** Evolution of the hydrological index *I* over time for target catchments for the period 1930 - 2030. The
783 points correspond to the dates where references of land-use sources are available (Table 2 and Fig. 8).

784

785

Hydrol. Earth Syst. Sci. Discuss., https://doi.org/10.5194/hess-2019-116
Manuscript under review for journal Hydrol. Earth Syst. Sci.
Discussion started: 2 May 2019

Hydrology and Earth System Sciences
Discussions

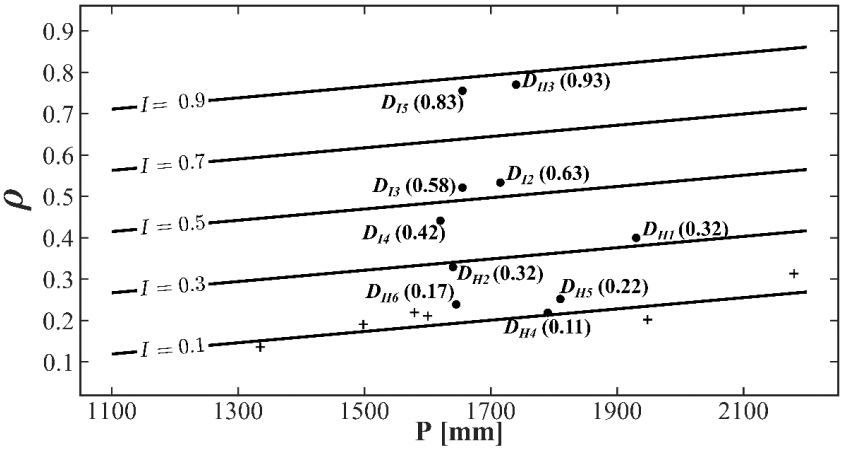

Figure 11. Abacus obtained from the model calibrated parameters for the relationship between annual runoff coefficient ρ and the annual precipitation P for different values of the hydrological index I. Each point corresponds to donor catchment; the value of the calculated hydrological index I (Table 3) is indicated into brackets. Crosses (+) correspond to available information at Etoa station between 1967 and 1983 for an unchanged hydrological index I estimated to 0.11.

Hydrol. Earth Syst. Sci. Discuss., https://doi.org/10.5194/hess-2019-116
Manuscript under review for journal Hydrol. Earth Syst. Sci.
Discussion started: 2 May 2019

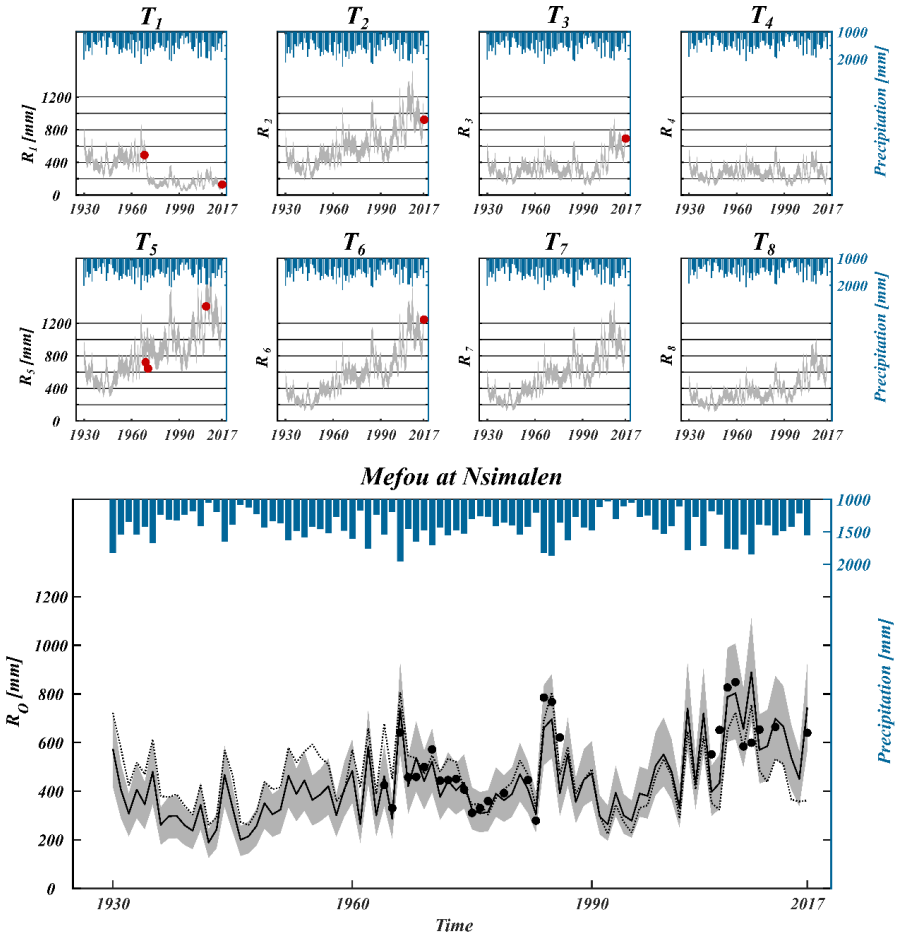

Figure 12. Annual runoff simulated on the 8 target catchments (T_1 to T_8) and on the Mefou catchment at Nsimalen for the period 1930-2017 (dark line with grey uncertainty range due to precipitation +/- 10 % and hydrological index I +/- 15 % estimation). The black points indicate the observed values on Nsimalen. The simulation with *GR1A* is presented with a dashed line.

Hydrol. Earth Syst. Sci. Discuss., https://doi.org/10.5194/hess-2019-116
Manuscript under review for journal Hydrol. Earth Syst. Sci.
Discussion started: 2 May 2019

Hydrology and Earth System Sciences
Discussions
Open Access
EGU

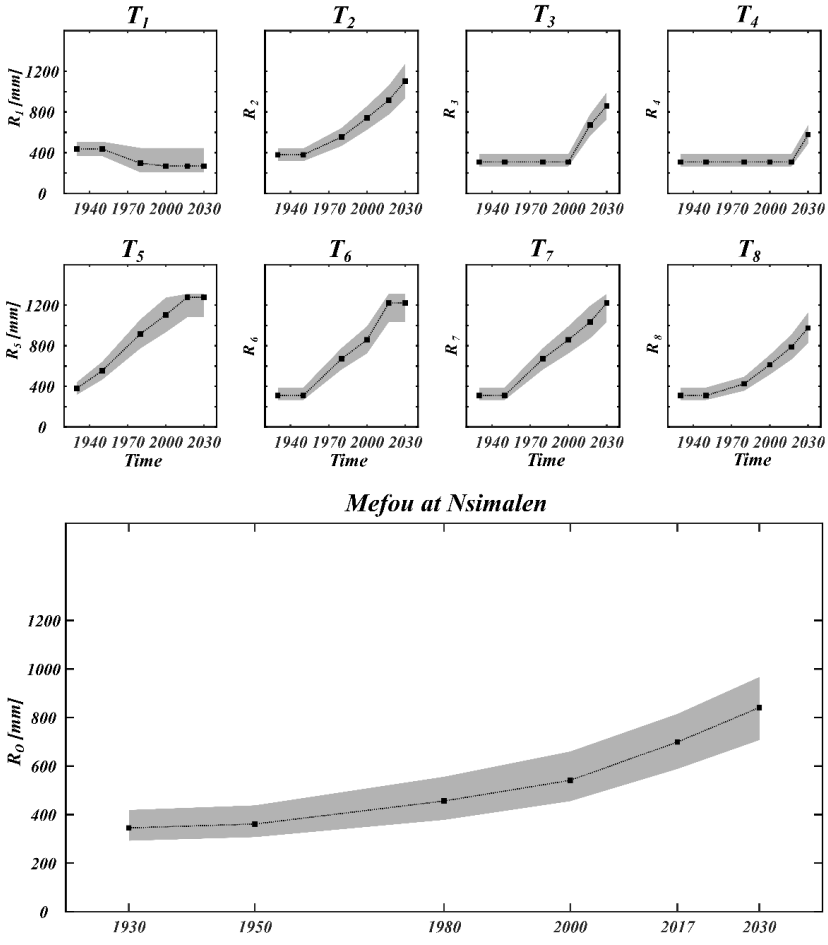

800

801 **Figure 13.** Simulated annual runoff for the target catchments (T_1 to T_8) and on the Mefou catchment at Nsimalen
802 for a reference precipitation $P_R = (P_n + P_x) / 2$ over the period 1930 – 2030 (dark line with grey uncertainty range
803 due to the hydrological index I +/- 15 % estimation).

804

Hydrol. Earth Syst. Sci. Discuss., https://doi.org/10.5194/hess-2019-116
Manuscript under review for journal Hydrol. Earth Syst. Sci.
Discussion started: 2 May 2019

805

Tables

Hydrol. Earth Syst. Sci. Discuss., https://doi.org/10.5194/hess-2019-116
Manuscript under review for journal Hydrol. Earth Syst. Sci.
Discussion started: 2 May 2019

Table 1. Characteristics of the donor catchments: name, reference, hydrometric station name, area, period of observation, annual precipitation *P*, annual runoff *R*, annual evapotranspiration *AET* = *P* - *R*, annual runoff coefficient ρ, the slope index S_I, the proportion of hydromorphic soil *HS*, and the proportion of urban areas *U*.

Name	*Reference*	*Hydrometric station*	*Area [km²]*	*Period*	*P [mm]*	*R[mm]*	*AET [mm]*	ρ	S_I *[%]*	*HS [%]*	*U [%]*
D_{H1}	Srang (1972)	MFOUNDI UPST	40	1970-71	1930	772	1158	0.40	11.5	0	5
D_{H2}	Srang (1972)	MFOUNDI UPST	40	1971-72	1640	540	1100	0.33	11.5	0	5
D_{H3}	Nguemou (2008)	MFOUNDI UPST	40	2006-07	1740	1340	400	0.77	11.5	0	> 75
D_{H4}	SNEC (1969)	ETOA	235	1968-69	1790	392	1398	0.22	9.0	44	< 1
D_{H5}	SNEC (1969)	MOPFOU	70	1968-69	1810	456	1354	0.25	13.5	0	< 1
D_{H6}	Ikounga (1978)	S3	24	1974-77	1645	393	1252	0.24	13.4	> 5	< 1
D_{I1}	Dedicated short-term instrumentation	MOPFOU	70	2017-18	1650	100	-	0.06	13.5	0	< 1
D_{I2}		MEFOU UPST	47	2017-18	1715	915	800	0.54 (0.53*)	13.6	3	46
D_{I3}		CANABOIS	120	2017-18	1655	863	792	0.47	10.0	6	28
D_{I4}		CANA-NKOM	73	2017-18	1620	712	908	0.44	10.0	8	9
D_{I5}		ECOPARK	21	2017-18	1655	1250	405	0.76	9.8	35	87
D_{I6}		ANGAA*	54	2017-18	575*	230*	-	0.40*	6.7	24	45

* The data on the Angaa catchment (D_{I6}) covers only the period from September to December. For comparison, the value of ρ is given for the same period for the Mefou Upstream (D_{I2}) which is characterized by similar value of *U*.

Hydrology and Earth System Sciences
Discussions
Open Access
EGU

Hydrol. Earth Syst. Sci. Discuss., https://doi.org/10.5194/hess-2019-116
Manuscript under review for journal Hydrol. Earth Syst. Sci.
Discussion started: 2 May 2019

Table 2. Reference studies, global products and resolution used to estimate each component (C_T, C_S *and* C_{LC}) of the index hydrological index *I* for 1930, 1950, 1980, 2000, 2017 and 2030. SRTM: Shuttle Radar Topography Mission 2014; *ESA CCI LC*: European Space Agency Climate Change Initiative Land Cover.

Type	*Period*	*References*	*Product*	*Spatial resolution*
Topography	*1930 - 2030*	SNEC (1969) Srang (1972) Ikounga (1978) Olivry (1979)	*SRTM 2014*	*30 m x 30 m*
Soil	*1930 - 2030*	Bachelier (1959) Humbel and Pellier (1969) Pellier (1969)	*SRTM 2014*	*30 m x 30 m*
Land-use	*1930*	Franqueville (1968, 1979)	*Population estimation*	-
	1950	Moffo (2016)	*Aerial photography*	-
	1980	Ebodé (2017)	*Landsat image*	-
		CUY (2008)	*Urban area map in* CUY (2008)	-
	2000	Midekisa et al. (2017) Moffo (2017)	*Map in* Midekisa et al. (2017)	*300 m x 300 m*
	2017	Midekisa et al. (2017)	*Map in* Midekisa et al. (2017)	*300 m x 300 m*
		Ebodé (2017)	*Landsat image*	-
	2030	UNDESA (2017)	*Prediction of population growth in* UNDESA (2017)	*By city and country*

Hydrol. Earth Syst. Sci. Discuss., https://doi.org/10.5194/hess-2019-116
Manuscript under review for journal Hydrol. Earth Syst. Sci.
Discussion started: 2 May 2019

Hydrology and Earth System Sciences
Discussions

Table 3. Characteristics of the three components C_T, C_S, C_{LC}, and the hydrological index I of the 12 donor catchments (Fig. 4b).

Name	C_T	C_S	C_{LC}	I
D_{H1}	0.50	1.00	0.20	0.32
D_{H2}	0.50	1.00	0.20	0.32
D_{H3}	0.50	1.00	1.00	0.94
D_{H4}	0.50	0.50	0.00	0.11
D_{H5}	1.00	1.00	0.00	0.22
D_{H6}	1.00	0.50	0.00	0.17
D_{I1}	1.00	1.00	0.00	0.22
D_{I2}	0.50	1.00	0.60	0.63
D_{I3}	0.50	0.50	0.60	0.58
D_{I4}	0.50	0.50	0.40	0.42
D_{I5}	0.50	0.00	1.00	0.83
D_{I6}	0.00	0.00	0.60	0.47

Hydrol. Earth Syst. Sci. Discuss., https://doi.org/10.5194/hess-2019-116
Manuscript under review for journal Hydrol. Earth Syst. Sci.
Discussion started: 2 May 2019

Hydrology and Earth System Sciences
Discussions
Open Access
EGU

818 **Table 4.** Characteristics of the 8 target catchments (Fig. 4b): area, the two components C_T, C_S and the dynamic
819 time variable component C_{LC} given in Fig. 8 (see references of land-use sources in Table 2).

Name	*Area [km²]*	C_T	C_S	C_{LC}					
				1930	*1950*	*1980*	*2000*	*2017*	*2030*
T_1	70	1.0	1.0	0.00	0.00	0.00	0.00	0.00	0.20
T_2	47	1.0	1.0	0.00	0.00	0.20	0.40	0.60	0.80
T_3	73	0.5	0.5	0.00	0.00	0.00	0.00	0.40	0.60
T_4	75	0.0	0.0	0.00	0.00	0.00	0.00	0.00	0.40
T_5	40	0.5	1.0	0.00	0.20	0.60	0.80	1.00	1.00
T_6	24	0.5	0.0	0.00	0.00	0.40	0.60	1.00	1.00
T_7	30	0.5	0.0	0.00	0.00	0.40	0.60	0.80	1.00
T_8	62	0.0	0.0	0.00	0.00	0.20	0.40	0.60	0.80

820

821

Hydrol. Earth Syst. Sci. Discuss., https://doi.org/10.5194/hess-2019-116
Manuscript under review for journal Hydrol. Earth Syst. Sci.
Discussion started: 2 May 2019

Hydrology and Earth System Sciences
Discussions

Table 5. Calculated values (either from observation or from model simulation as indicated) of *R*, *ρ*, *AET*, and *K* for each target catchments and for the whole Mefou catchment at Nsimalen taking into account +/- 10 % uncertainty on *P* and +/- 15 % *I* for the hydrological year 2017-2018.

Catch. Name	***Method***	***P [mm]***	***R [mm]***	***AET [mm]***	***ρ***	***K [%]***
T_1	*Obs. (D_{I1})*	*1500*	*100 ± 25*	*-*	*-*	*2.5*
T_2	*Obs. (D_{I2})*	*1715*	*915 ± 90*	*800*	*0.53*	*15.0*
T_3	*Obs. (D_{I3})*	*1620*	*715 ± 75*	*905*	*0.43*	*18.5*
T_4	*Sim.*	*1660*	*370 ± 75*	*1290*	*0.24*	*9.0*
T_5	*Sim.*	*1620*	*1230 ± 125*	*390*	*0.76*	*18.0*
T_6	*Obs. (D_{I5})*	*1655*	*1130 ± 125*	*525*	*0.68*	*10.0*
T_7	*Sim.*	*1650*	*1030 ± 200*	*620*	*0.62*	*11.0*
T_8	*Sim.*	*1580*	*730 ± 150*	*775*	*0.46*	*16.0*
Mefou	*Sum of volumes of T_i*	*1650*	*660 ± 65*	*990*	*0.41*	*100*

Hydrol. Earth Syst. Sci. Discuss., https://doi.org/10.5194/hess-2019-116
Manuscript under review for journal Hydrol. Earth Syst. Sci.
Discussion started: 2 May 2019

826 **Table 6.** Mean values of P, R, ρ, and percentile Q_{95} and Q_5 for 1950-1980 and 1987-2017 for the eight sub-catchments and the whole catchment.

	1950 - 1980					1987 - 2017					Changes				
Name	$\overline{P}$ **[mm]**	$\overline{R}$ **[mm]**	$\overline{\rho}$	Q_{95} **[mm]**	Q_5 **[mm]**	$\overline{P}$ **[mm]**	$\overline{R}$ **[mm]**	$\overline{\rho}$	Q_{95} **[mm]**	Q_5 **[mm]**	$\overline{P}$ **[%]**	$\overline{R}$ **[%]**	$\overline{\rho}$ **[%]**	Q_{95} **[%]**	Q_5 **[%]**
T_1	-	356	-	-	-	-	144	-	-	-	-	-	-	-	-
T_2	1706	529	0.31	803	346	1628	803	0.48	1255	454	- 5	+52	+58	+56	+31
T_3	1625	324	0.20	528	200	1550	405	0.25	783	149	- 5	+25	+28	+48	-26
T_4	1625	324	0.20	528	200	1550	297	0.19	508	149	- 5	-8	-6	-4	-26
T_5	1625	764	0.47	1108	503	1550	1104	0.70	1627	690	- 5	+45	+50	+47	+37
T_6	1625	477	0.29	743	276	1550	852	0.54	1352	461	- 5	+79	+85	+82	+67
T_7	1625	434	0.27	678	247	1550	741	0.47	1143	429	- 5	+71	+77	+69	+74
T_8	1544	315	0.20	502	197	1473	511	0.34	846	256	- 5	+62	+69	+69	+30
Mefou	1625	409	0.25	650	280	1550	518	0.33	840	273	-5	+27	+31	+29	-2

827

Hydrology and Earth System Sciences
Discussions
Open Access
EGU

Hydrol. Earth Syst. Sci. Discuss., https://doi.org/10.5194/hess-2019-116
Manuscript under review for journal Hydrol. Earth Syst. Sci.
Discussion started: 2 May 2019

Hydrology and Earth System Sciences
Discussions

Appendix A

List of Notations

A	:	Parameter of the equation: $\rho = AP + B$ [-]
A_i	:	Area of target sub-catchment i [L^2]
A_O	:	Area of the whole catchment [L^2]
a	:	Parameter of the model in $\rho_D = aI + b$ [-]
AET	:	Annual evapotranspiration [L]
B	:	Parameter of the equation: $\rho = AP + B$ [-]
b	:	Second parameter of the model in $\rho_D = aI + b$ [-]
C_i	:	Component i of the hydrological index [-]
C_{LC}	:	Land-use component of the hydrological index I [-]
C_S	:	Soil component of the hydrological index I [-]
C_T	:	Topographic component of the hydrological index I [-]
CN	:	Curve Number in SCS method
D	:	Donor catchments [-]
D_{Ii}	:	Donor catchment i from dedicated short-term instrumentation [-]
D_{Hi}	:	Donor catchment i from historical database [-]
E	:	Normalized Error (Eq. 10) [-]
$\bar{E}$	:	Mean Absolute Normalized Error (Eq. 11) [-]
G	:	Term defined in Eq 16 [-]
HS	:	Proportion of hydromorphic soil [-]
I	:	Hydrological index [-]
I_n	:	Maximum value of I [-]
I_x	:	Minimum value of I [-]
K_i	:	Contribution of sub-catchment i to the whole catchment ($K_i = V_i / V_O$) [-]

854	P	:	Annual precipitation [L]
855	P_m	:	Mean annual precipitation over the historical database [L]
856	P_n	:	Minimal annual precipitation over the historical database [L]
857	P_R	:	Reference annual precipitation corresponding to $P_R = \frac{P_x+P_n}{2}$ [L]
858	P_{Ti}	:	Annual precipitation of target catchment *i* (Eq. 12) [L]
859	P_x	:	Maximal annual precipitation over the historical database [L]
860	$\bar{P}$	:	Mean annual precipitation for a period of 30 years (1950-1980 and 1987-2017)
861	P_1	:	Annual precipitation at historical raingauge P_1 [L]
862	P_2	:	Annual precipitation at historical raingauge P_2 [L]
863	PET	:	Potential evapotranspiration [L]
864	Q_5	:	Annual runoff corresponding to the 5th-percentile over a period of 30 years [L]
865	Q_{95}	:	Annual runoff corresponding to the 95th-percentile over a period of 30 years [L]
866	R	:	Annual Runoff [L]
867	R_i	:	Annual Runoff of target sub-catchment *i* [L]
868	R_O	:	Annual Runoff of the whole catchment [L]
869	$\bar{R}$	:	Mean annual simulated runoff for a period of 30 years (1950-1980 and 1987-2017)
870	r^2	:	Coefficient of determination (Eq. 9)
871	$RMSE$	:	Roots Mean Square Error [L]
872	S_i	:	Slope index [%]
873	T_i	:	Target sub-catchment *i* [-]
874	U	:	Proportion of urbanized area [%]
875	V_i	:	Annual volume at sub-catchment *i* [L^3]
876	V_O	:	Annual volume at the whole catchment [L^3]
877			
878	β_1	:	Parameter of the model ($\beta_1 = \rho_{x,1} - \rho_{n,1}$) [-]
879	β_2	:	Constant characteristic ($\beta_2 = \rho_{x,P} - \rho_{n,P}$)
880	ρ	:	Annual runoff coefficient [-]

$\bar{\rho}$	:	Mean simulated annual runoff coefficient for a period of 30 years (1950-1980 and 1987-2017) [-]
ρ_D	:	Simulated annual runoff coefficient from donors regression: $\rho_D = aI + b$ [-]
$\rho_{n,I}$	:	ρ for P_n and I [-]
$\rho_{n,P}$	:	ρ for I_n and P [-]
$\rho_{x,I}$	:	ρ for P_x and I [-]
$\rho_{x,P}$	:	ρ for I_x and P [-]
ω_i	:	Weight attributed to the component i of the hydrological index in Eq. 7 [-]
ω_{LC}	:	Weight attributed to the land-use component of the hydrological index [-]
ω_S	:	Weight attributed to the soil component of the hydrological index [-]
ω_T	:	Weight attributed to the topographic component of the hydrological index [-]

List of abbreviations

CUY	:	Communauté Urbaine de Yaoundé
ESA CCI LC	:	European Space Agency Climate Change Initiative
IAHS	:	International Association of Hydrological Sciences
LULC	:	Land-Use Land-Cover
PUB	:	Prediction in Ungauged Basins
SCS	:	Soil Conservation Services
SNEC	:	Société Nationale des Eaux du Cameroun
SRTM	:	Shuttle Radar Topography Mission
UNDESA	:	United Nations Department of Economic and Social Affairs

Hydrol. Earth Syst. Sci. Discuss., https://doi.org/10.5194/hess-2019-116
Manuscript under review for journal Hydrol. Earth Syst. Sci.
Discussion started: 2 May 2019

References

Abbott, M.B., Bathurst, J.C., Cunge, J.A., O'Connell, P.E., Rasmussen, J.: An introduction to the European Hydrological System — Systeme Hydrologique Europeen, "SHE", 1: History and philosophy of a physically-based, distributed modelling system. Journal of Hydrology 87, 45–59. https://doi.org/10.1016/0022-1694(86)90114-9. 1986.

Bachelier, G.: Etude pédologique des sols de Yaoundé : Contribution à l'étude de la pédogenèse des sols ferrallitiques. Agronomie Tropicale 14, 279–305. 1959.

Barron, O.V., Barr, A.D., Donn, M.J. Effect of urbanisation on the water balance of a catchment with shallow groundwater. Journal of Hydrology, Hydrology of peri-urban catchments: processes and modelling 485, 162–176. https://doi.org/10.1016/j.jhydrol.2012.04.027. 2013.

Bagarello, V., Prima, S.D., Iovino, M., Provenzano, G.: Estimating field-saturated soil hydraulic conductivity by a simplified Beerkan infiltration experiment. Hydrological Processes 28, 1095–1103. https://doi.org/10.1002/hyp.9649. 2014.

Beck, H.E., Bruijnzeel, L.A., van Dijk, A.I.J.M., McVicar, T.R., Scatena, F.N., Schellekens, J.: The impact of forest regeneration on streamflow in 12 mesoscale humid tropical catchments. Hydrol. Earth Syst. Sci. 17, 2613–2635. https://doi.org/10.5194/hess-17-2613-2013. 2013

Beauvais, A.: Geochemical mass balance of lateritization processes and climatic change signatures in weathering profiles overlain by ferricretes in Central Africa. Geochim. Cosmochim.Acta 63, 3939–3957.1999.

Beighley, R.E., Melack, J.M., Dunne, T.: Impacts of California's Climatic Regimes and Coastal Land Use Change on Streamflow Characteristics1. JAWRA Journal of the American Water Resources Association 39, 1419–1433. https://doi.org/10.1111/j.1752-1688.2003.tb04428.x. 2003.

Bergström, S. and Singh, V.: The HBV Model. In: Singh, V.P., Ed., Computer Models of Watershed Hydrology, Water Resources Publications, Highlands Ranch, 443-476. 1995:

Bilong, P., Eno Belinga S. M. and Volkoff B.: Séquence d'évolution des paysages cuirassés et des sols ferrallitiques en zones forestières tropicales d'Afrique Centrale: place des sols à horizons d'argiles tachetées. C. R. Acad. Sci. Paris 314, 109–115. 1992.

Bitom, D., Volkoff B., Beauvais A., Seyler F. and Ndjigui P.-D.: Rôle des héritages latéritiques et du niveau des nappes dans l'évolution des modelés et des sols en zone intertropicale forestière humide. C. R. Acad. Sci. Paris 336, 1161–1170. 2004.

Blöschl, G. (Ed.): Runoff prediction in ungauged basins: synthesis across processes, places and scales. Cambridge University Press, Cambridge. 2013.

Bopda, A.: *Yaoundé et le défi camerounais de l'intégration. À quoi sert une capitale d'Afrique tropicale?* Paris, CNRS Editions, 422 p. 2003

Branchet, P., Cadot, E., Fenet, H., Sebag, D., Ngatcha, B.N., Borrell-Estupina, V., Ngoupayou, J.R.N., Kengne, I., Braun, J.-J., Gonzalez, C.: Polar pesticide contamination of an urban and peri-urban tropical watershed affected by agricultural activities (Yaoundé, Center Region, Cameroon). Environmental Science and Pollution Research 25, 17690–17715. https://doi.org/10.1007/s11356-018-1798-4. 2018.

Braud, I., Breil, P., Thollet, F., Lagouy, M., Branger, F., Jacqueminet, C., Kermadi, S., Michel, K.: Evidence of the impact of urbanization on the hydrological regime of a medium-sized periurban catchment in France. Journal of Hydrology 485, 5–23. https://doi.org/10.1016/j.jhydrol.2012.04.049. 2013

Braun, J.-J., Marechal, J.-C., Riotte, J., Boeglin, J.-L., Bedimo Bedimo, J.-P., Ndam Ngoupayou, J.R., Nyeck, B., Robain, H., Sekhar, M., Audry, S., Viers, J.: Elemental weathering fluxes and saprolite production rate in a Central African lateritic terrain (Nsimi, South Cameroon). Geochimica et Cosmochimica Acta 99, 243–270. https://doi.org/10.1016/j.gca.2012.09.024. 2012

Braun, J.-J., Ngoupayou, J.R.N., Viers, J., Dupre, B., Bedimo Bedimo, J.-P., Boeglin, J.-L., Robain, H., Nyeck, B., Freydier, R., Nkamdjou, L.S., Rouiller, J., Muller, J.-P.: Present weathering rates in a humid tropical

watershed: Nsimi, South Cameroon. Geochimica et Cosmochimica Acta 69, 357–387. https://doi.org/10.1016/j.gca.2004.06.022. 2005

Budyko, M.I.: Climate and life, Academic Press, Orlando, FL, 508 pp. 1974.

Crabit, A., Colin, F., Moussa, R.: A soft hydrological monitoring approach for comparing runoff on a network of small poorly gauged catchments. Hydrological Processes 25, 2785–2800. https://doi.org/10.1002/hyp.8041. 2011.

CUY.: *Schéma directeur d'Aménagement Urbain : Yaoundé 2020.* Communauté Urbaine de Yaoundé, International AUGEA, 120p. 2008.

Daily, G.C.: Nature's Services: Societal Dependence On Natural Ecosystems. Island Press. 1997.

Ebodé, V.B.: Etude de la variabilité hydroclimatique dans un bassin versant forestier en voie d'urbanisation accélérée : Le cas de la Mefou. Mém., Master. Univ. Yaoundé I. 156p. 2017.

Franqueville, A.: Le paysage urbain de Yaoundé. sn, sl, 39p. 1968.

Franqueville, A.: Croissance démographique et immigration à Yaoundé. Les Cahiers d'Outre-Mer 32, 321–354. https://doi.org/10.3406/caoum.1979.2914. 1979.

Genwei, C.: Forest Change: Hydrological Effects in the Upper Yangtze River Valley. Ambio 28, 457–459. 1999

Gessesse, B., Bewket, W., Bräuning, A.: Model-Based Characterization and Monitoring of Runoff and Soil Erosion in Response to Land Use/land Cover Changes in the Modjo Watershed, Ethiopia: Runoff and Soil Erosion in Response to Land Use/Land Cover Flux. Land Degradation & Development 26, 711–724. https://doi.org/10.1002/ldr.2276. 2015.

Güneralp, B., Lwasa, S., Masundire, H., Parnell, S., Seto, K.: Urbanization in Africa: Challenges and opportunities for conservation. Environmental Research Letters 13. https://doi.org/10.1088/1748-9326/aa94fe. 2017.

Gupta, A.: Observations on the Effects of Urbanization on Runoff and Sediment Production in Singapore. Singapore Journal of Tropical Geography 3, 137–146. https://doi.org/10.1111/j.1467-9493.1982.tb00236.x. 1982.

Hughes, D.A., Jewitt, G., Mahé, G., Mazvimavi, D., Stisen, S.: A review of aspects of hydrological sciences research in Africa over the past decade. Hydrological Sciences Journal 1–15. https://doi.org/10.1080/02626667.2015.1072276. 2015.

Humbel, F.-X., Pellier, J.L.: Porosité, densité et perméabilité de sols ferrallitiques rouge et jaune près de Yaoundé. ORSTOM, Yaoundé, 28p. 1969.

Ikounga, M. Analyse fine du mécanisme de la formation du ruissellement sur sols ferrallitiques sous forêt (région de Yaoundé-Cameroun). ORSTOM, Paris. 1978.

Janicot, S., Reinert, M., Institut de recherche pour le développement (France) (Eds.): Changement climatique: quels défis pour le Sud? IRD éditions, Marseille. 268p. 2015.

Koutsoyiannis, D.: Hydrology and change. Hydrological Sciences Journal 58, 1177–1197. https://doi.org/10.1080/02626667.2013.804626. 2013.

Krasovskaia, I.: A Study of Mesoscale Runoff Variability. Geografiska Annaler. Series A, Physical Geography 70, 191. https://doi.org/10.2307/521071. 1988.

Kundzewicz, Z.W., Mata, L.J., Arnell, N.W., Doll, P., Kabat, P., Jimenez, B., Miller, K., Oki, T., Zekai, S., Shiklomanov, I.: Freshwater resources and their management, in: Parry, M.L., Canziani, O.F., Palutikof, J.P., van der Linden, P.J., Hanson, C.E. (Eds.), Climate Change 2007: Impacts, Adaptation and Vulnerability. Contribution of Working Group II to the Fourth Assessment Report of the Intergovernmental Panel on Climate Change. Cambridge University Press, pp. 173–210. 2007.

Le Coz, J., Patalano, A., Collins, D., Guillén, N.F., García, C.M., Smart, G.M., Bind, J., Chiaverini, A., Le Boursicaud, R., Dramais, G., Braud, I.: Crowdsourced data for flood hydrology: Feedback from recent citizen science projects in Argentina, France and New Zealand. Journal of Hydrology 541, 766–777. https://doi.org/10.1016/j.jhydrol.2016.07.036. 2016.

998 Le Moine, N.: Le bassin versant de surface vu par le souterrain : une voie d'amélioration des performances et du
999 réalisme des modèles pluie-débit? PhD thesis, Université Paris VI Pierre et Marie Curie, Paris, France.
1000 2008.

1001 Lefèvre, R.: Etude hydrologique de la Mefou supérieure. ORSTOM, Yaoundé, 38p. 1966.

1002 Lowry, C.S., Fienen, M.N.: CrowdHydrology: Crowdsourcing Hydrologic Data and Engaging Citizen Scientists.
1003 Ground Water 51, 151–156. https://doi.org/10.1111/j.1745-6584.2012.00956.x. 2013.

1004 Maréchal, J.-C., Braun, J.-J., Riotte, J., Bedimo, J.-P.B., Boeglin, J.-L.: Hydrological processes of a rainforest
1005 headwater swamp from natural chemical tracing in Nsimi watershed, Cameroon. Hydrological Processes
1006 25, 2246–2260. https://doi.org/10.1002/hyp.7989. 2011.

1007 Mazzoleni, M., Verlaan, M., Alfonso, L., Monego, M., Norbiato, D., Ferri, M., Solomatine, D.P.: Can assimilation
1008 of crowdsourced data in hydrological modelling improve flood prediction? Hydrology and Earth System
1009 Sciences 21, 839–861. https://doi.org/10.5194/hess-21-839-2017. 2017.

1010 McMillan, H., Montanari, A., Cudennec, C., Savenije, H., Kreibich, H., Krueger, T., Liu, J., Mejia, A., Van Loon,
1011 A., Aksoy, H., Di Baldassarre, G., Huang, Y., Mazvimavi, D., Rogger, M., Sivakumar, B., Bibikova, T.,
1012 Castellarin, A., Chen, Y., Finger, D., Gelfan, A., Hannah, D.M., Hoekstra, A.Y., Li, H., Maskey, S.,
1013 Mathevet, T., Mijic, A., Pedrozo Acuña, A., Polo, M.J., Rosales, V., Smith, P., Viglione, A., Srinivasan,
1014 V., Toth, E., van Nooyen, R., Xia, J.,. Panta Rhei 2013–2015: global perspectives on hydrology, society
1015 and change. Hydrological Sciences Journal 1–18. https://doi.org/10.1080/02626667.2016.1159308.
1016 2016.

1017 Midekisa, A., Holl, F., Savory, D.J., Andrade-Pacheco, R., Gething, P.W., Bennett, A., Sturrock, H.J.W.: Mapping
1018 land cover change over continental Africa using Landsat and Google Earth Engine cloud computing.
1019 PLoS One 12. https://doi.org/10.1371/journal.pone.0184926. 2017.

1020 Mishra, S.K., Singh, V.P.: Soil Conservation Service Curve Number (SCS-CN) Methodology, Water Science and
1021 Technology Library. Springer Netherlands, Dordrecht. https://doi.org/10.1007/978-94-017-0147-1.
1022 2003.

1023 Moffo, Z.M.: Contribution des systèmes d'information géographique pour la cartographie des zones à risques
1024 d'inondation à Yaoundé : Application au bassin versant du Mfoundi., Mém. Master. 71p. 2017.

1025 Montanari, A., Young, G., Savenije, H.H.G., Hughes, D., Wagener, T., Ren, L.L., Koutsoyiannis, D., Cudennec,
1026 C., Toth, E., Grimaldi, S., Blöschl, G., Sivapalan, M., Beven, K., Gupta, H., Hipsey, M., Schaefli, B.,
1027 Arheimer, B., Boegh, E., Schymanski, S.J., Di Baldassarre, G., Yu, B., Hubert, P., Huang, Y., Schumann,
1028 A., Post, D.A., Srinivasan, V., Harman, C., Thompson, S., Rogger, M., Viglione, A., McMillan, H.,
1029 Characklis, G., Pang, Z., Belyaev, V.: "Panta Rhei—Everything Flows": Change in hydrology and
1030 society—The IAHS Scientific Decade 2013–2022. Hydrological Sciences Journal 58, 1256–1275.
1031 https://doi.org/10.1080/02626667.2013.809088. 2013.

1032 Mouelhi, S.: Vers une chaîne cohérente de modèles pluie-débit conceptuels globaux aux pas de temps pluriannuel,
1033 annuel, mensuel et journalier (thesis). Paris, ENGREF. 2003.

1034 Mouelhi, S., Michel, C., Perrin, C., Andréassian, V.: Linking stream flow to rainfall at the annual time step: The
1035 Manabe bucket model revisited. Journal of Hydrology 328, 283–296.
1036 https://doi.org/10.1016/j.jhydrol.2005.12.022. 2006.

1037 Moussa, R., Lhomme, J.-P.: The Budyko functions under non-steady-state conditions. Hydrology and Earth
1038 System Sciences 20, 4867–4879. https://doi.org/10.5194/hess-20-4867-2016. 2016.

1039 Nguemou, T.D.: Hydrologie et transports solides dans un écosystème forestier urbanisé: Exemple du
1040 bassin versant du Mfoundi au centre sud du Cameroun. Mém. DEA. Fac des sci. Yaoundé I. 83p. 2008.

1041 Ngoumdoum, D.F.: Hydrologie et qualité des eaux de surface du bassin versant élémentaire d'Odza (Yaoundé,
1042 Cameroun). Mém. Master, Univ. Yaoundé I. Fac. Sci. DST. 70p. 2013.

1043 Olivry, J.-C.: Monographie du Nyong et des fleuves cotiers : T.I.: Facteurs conditionnels des régimes
1044 hydrologiques. T.2: Hydrologie du Nyong. T.3: Hydrologie des fleuves cotiers. ONAREST, Yaoundé.
1045 523 p.. 1979.

1046 Parajka, J., Viglione, A., Rogger, M., Salinas, J.L., Sivapalan, M., Blöschl, G.: Comparative assessment of
1047 predictions in ungauged basins – Part 1: Runoff-hydrograph studies. Hydrology and Earth
1048 System Sciences 17, 1783–1795. https://doi.org/10.5194/hess-17-1783-2013. 2013.

1049 Pellier, J.L.: Données générales sur la répartition des principaux types de sols de la région de Yaoundé. Yaoundé:
1050 ORSTOM, 24 p. 1969.

1051 Ponce, V.M., Shetty, A.V.: A conceptual model of catchment water balance: 1. Formulation and calibration.
1052 Journal of Hydrology 173, 27–40. https://doi.org/10.1016/0022-1694(95)02739-C. 1995.

1053 Roche, M.: Hydrologie de surface. Gauthier-Villars, Paris, 430p. 1963.

1054 Russo, K.A., Smith, Z.A.: The Millennium Ecosystem Assessment, in: Russo, K.A., Smith, Z.A. (Eds.), What
1055 Water Is Worth: Overlooked Non-Economic Value in Water Resources. Palgrave Macmillan US, New
1056 York, pp. 39–51. https://doi.org/10.1057/9781137062499_3. 2013.

1057 Salinas, J.L., Laaha, G., Rogger, M., Parajka, J., Viglione, A., Sivapalan, M., Blöschl, G.: Comparative assessment
1058 of predictions in ungauged basins – Part 2: Flood and low flow studies. Hydrology and Earth
1059 System Sciences 17, 2637–2652. https://doi.org/10.5194/hess-17-2637-2013. 2013.

1060 SCS : In Hydrology, National Engineering of Handbook, Soil Conservation Service. Supplement A, Section 4,
1061 Chap. 10, USDA, Washington DC. 1956.

1062 Sivapalan, M., Yaeger, M.A., Harman, C.J., Xu, X., Troch, P.A.: Functional model of water balance variability at
1063 the catchment scale: 1. Evidence of hydrologic similarity and space-time symmetry: Space-time
1064 symmetry of water variability. Water Resources Research 47. https://doi.org/10.1029/2010WR009568.
1065 2011.

1066 SNEC : Barrage de Mopfou amont : Etude hydrologique de la Méfou supérieure campagne 1968-1969. EDF-
1067 Igeco, Paris, 64p. 1969.

1068 SRTM : Shuttle Radar Topography Mission, hydrographic network. https://www2.jpl.nasa.gov/srtm/, Accessed
1069 date: 11 December 2018. 2014.

1070 Srang, K.: Hydrologie d'un bassin de zone urbaine : le Bassin versant de Yaoundé. ORSTOM, Yaoundé, 53p.
1071 1972.

1072 Turc, L.: Le bilan d'eau des sols: relations entre les précipitations, l'évaporation et l'écoulement, Annales
1073 Agronomiques, Série A(5), 491–595. 1954.

1074 UNDESA : World Population Prospects: The 2017 Revision, Key Findings and Advance Tables. 2017.

1075 Wagner, P.D., Kumar, S., Schneider, K.: An assessment of land use change impacts on the water resources of the
1076 Mula and Mutha Rivers catchment upstream of Pune, India. Hydrology and Earth System Sciences 17,
1077 2233–2246. https://doi.org/10.5194/hess-17-2233-2013. 2013.

1078 White, M.D., Greer, K.A. The effects of watershed urbanization on the stream hydrology and riparian vegetation
1079 of Los Peñasquitos Creek, California. Landscape and Urban Planning 74, 125–138.
1080 https://doi.org/10.1016/j.landurbplan.2004.11.015. 2006.

1081 Yira, Y., Diekkrüger, B., Steup, G., Bossa, A.Y.: Modeling land use change impacts on water resources in a
1082 tropical West African catchment (Dano, Burkina Faso). Journal of Hydrology 537, 187–199.
1083 https://doi.org/10.1016/j.jhydrol.2016.03.052. 2016.

1084 Zhou, G., Wei, X., Luo, Y., Zhang, M., Li, Y., Qiao, Y., Liu, H., Wang, C.: Forest recovery and river discharge at
1085 the regional scale of Guangdong Province, China: Forest recovery and river discharge. Water Resources
1086 Research 46. https://doi.org/10.1029/2009WR008829. 2010.

1087 Zhou, G., Wei, X. Chen, X., Zhou, P., Liu, X., Xiao, Y., Sun, G., Scott, D.F., Zhou, S, Han, L., Su, Y.: Global
1088 pattern for the effect of climate and land cover on water yield. Nature Communications 6:5918,
1089 https://doi.org/10.1038/ncomms6918. 2015.

1090